solar cells in the face of radiation-induced carrier-lifetime degradation. More recently it has been realized that some parallel multiple-vertical-junction structures, such as shown in Fig. 11.3*a*, can have exceedingly small series resistance (Frank, 1980). Figure 11.3*b* shows the measured efficiency and projected efficiency after further development on the antireflection coating and reduction of light obstruction.

Series Multiple-Vertical-Junction Cell

A concentrator Si solar cell operating under a 0.1-m^2 lens would be a power source of about 10 W at 0.6 V and 16 A. This is a somewhat inconvenient combination of low voltage and high current for interconnection or use. If the cell consisted of 16 cells in series, the cell voltage and current would be, more agreeably, 9.6 V and 1 A. A simple structure that provides the series structure is shown in Fig. 11.4. Wafers with diffused *pn* junctions are stacked and interleaved with thin aluminum foil. The stack is sintered under compression to form a solid block of serially connected *pn*-junction diodes. The block can be sliced lengthwise to yield multiple-junction solar cells (Sater, 1975). This technology is standard for producing very high voltage rectifiers. There has not been much effort in demonstrating high cell efficiency.

Series multiple-junction designs eliminate the high current and thus the series resistance limitations. One disadvantage of this and all other series multiple-junction cells is that they are sensitive to the nonuniformity of light intensity. The cell current is the smallest of the short-circuit currents of all the subcells.

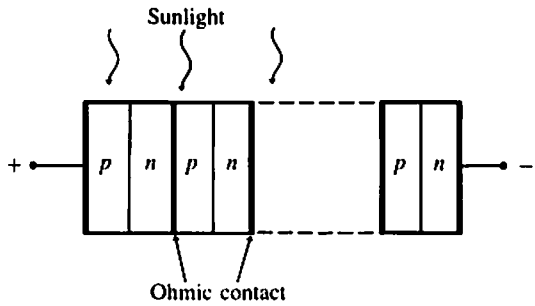

Figure 11.4 A cell having many junctions connected in series produces relatively high voltage and low current—a combination that is often desirable. However, series multiple junction cells perform well only if all junctions are illuminated at the same intensity.

V-Groove Multijunction (VGMJ) Solar Cell

This is another series multiple-junction structure. It is made with a novel manufacturing process and provided with an integral glass front cover (Chappell, 1978). Figure 11.5*a* illustrates the fabrication steps. The oxidized p or n Si wafer is bonded to a glass plate by a known electro-thermal bonding technique (see Sec. 9.5). Anisotropic etching, described in Sec. 4.3, is used to isolate Si into islands with V-shaped grooves. Shadowing by the neighboring islands and the oxide overhang allows n^+ and p^+ regions to be ion-implanted as well as makes possible the interconnection of the neighboring islands. Figure 11.5*b* shows the calculated efficiency of this cell.

Interdigitated-Back-Contact (IBC) Cell

The structure of this cell is shown in Fig. 11.6*a* (Schwartz, 1975). The elimination of front contacts completely removes the trade-off between contact shadowing and series resistance. In this structure, the main contribution of series resistance is from the bulk material of the cell. At high intensities, conductivity modulation makes the series resistance decrease in almost inverse proportion to the intensity. This is true for all the concentrator cells discussed in this section. The interdigitated contacts do aggravate the problem of cooling the cell to some degree. Low surface recombination velocity and long diffusion length are of critical importance to this cell and the VGMJ cell.

High-Low Junction Emitter Cell

It was pointed out in Chap. 3 that the heavily doped region of a silicon solar cell presents several problems such as very short carrier lifetime and low effective doping density. There is some experimental evidence that with the base of an n^+p solar cell doped to 0.1 $\Omega \cdot$ cm, the hole injection current into the n^+ region is 10 times the electron injection current into the p-type base. A high-low junction emitter structure has been proposed to curb the hole injection into the n^+ layer (Sah, 1978). The new structure has an n^+np configuration. The n^+ layer has the usual 0.25 μm thickness; the n layer is several microns thick. Depending on the doping concentration in the n layer, high-level injection occurs in this layer at solar concentration ratios of one to ten. When high-level injection occurs, the electron and hole densities in the

---

Figure 11.5 (*a*) Steps of making a V-groove multijunction cell. Step 1: grow SiO_2 layer, bond oxidized wafer to glass, etch V-groove pattern windows in SiO_2. Step 2: V-groove etch Si down to glass, ion implant n^+ and p^+ regions, anneal. Step 3: Deposit metal and alloy. (*b*) Calculated efficiency. (*Chappel, 1978.*)

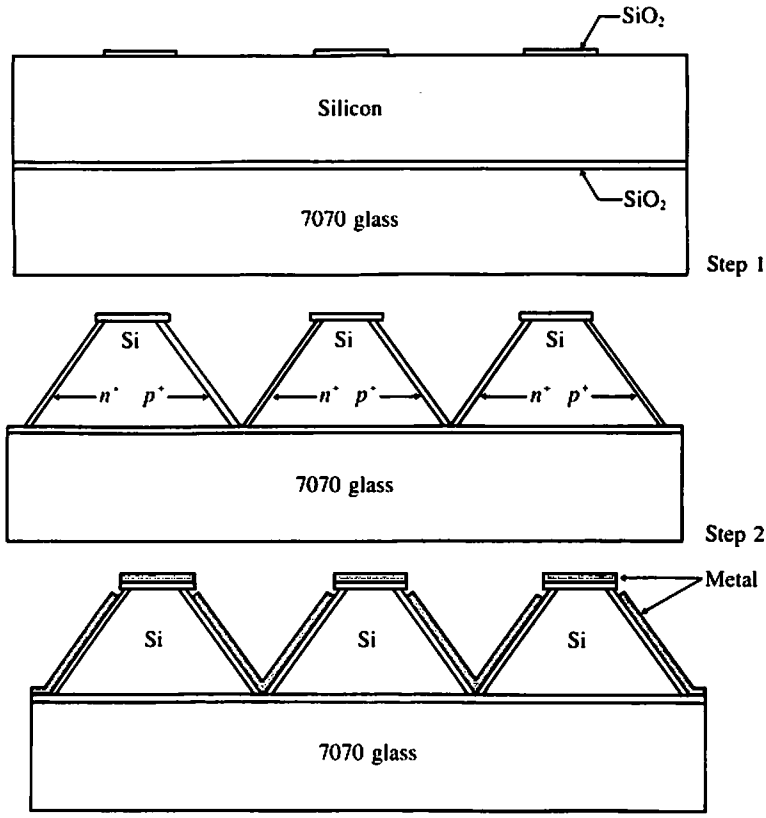
SiO2
Silicon
SiO2
7070 glass
Step 1
Si
Si
Si
n+ p+
n+ p+
n+ p+
7070 glass
Step 2
Metal
Si
Si
Si
7070 glass
Step 3

(*a*)

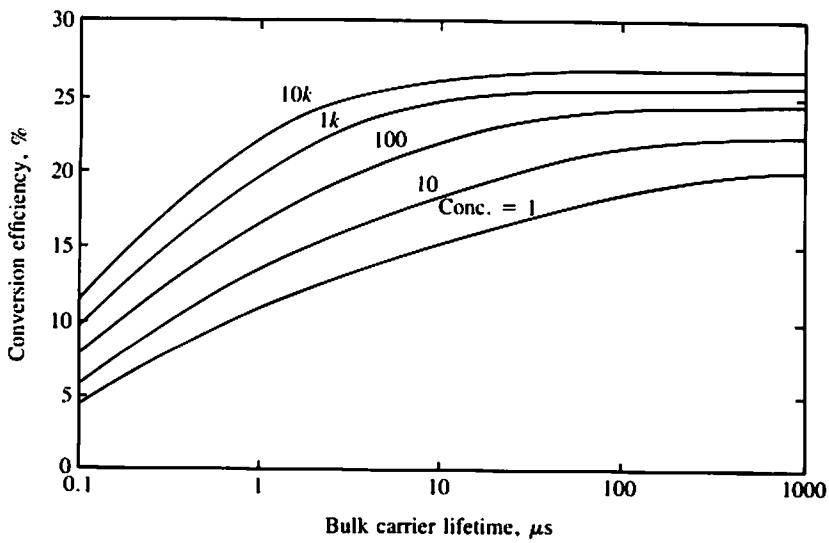
30
25
20
15
10
5
0
0.1
1
10
100
1000
10k
1k
100
10
Conc. = 1
Conversion efficiency, %
Bulk carrier lifetime, μs

(*b*)

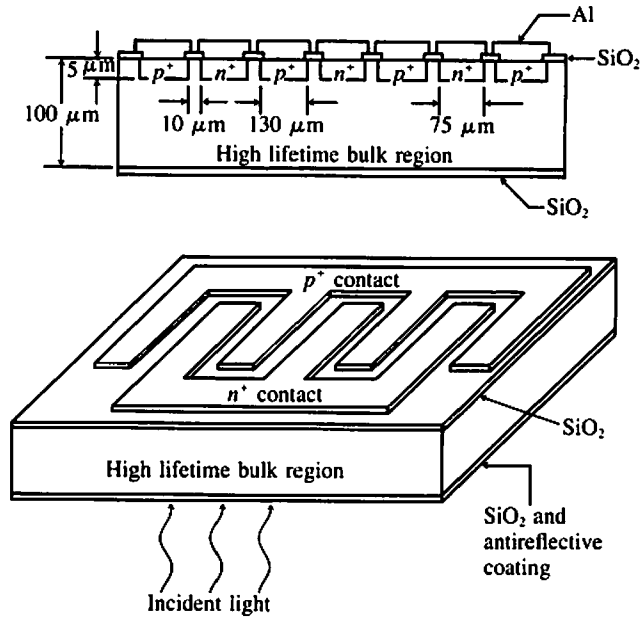

(*a*)

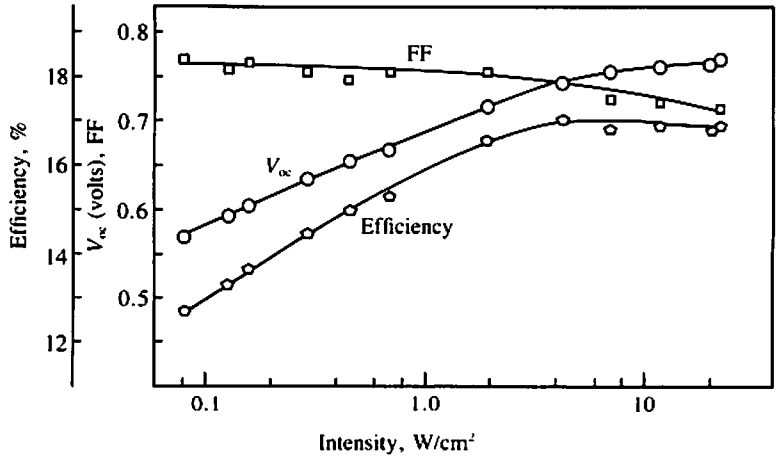

(*b*)

Figure 11.6 (*a*) Structure and (*b*) performance of interdigitated back contact cell. (*Schwartz, 1975.*)

Table 11.1 Calculated performance of high-low junction emitter cell (n layer is 10 μm thick doped to 1×10^{14} cm^{-3}) and conventional cell

Base resistivity is 0.1 $\Omega \cdot$ cm

	1 sun			
	J_{sc}, A/cm^2	V_{oc}, V	FF	η, %
High-low junction emitter (n^+np)	0.031	0.626	0.804	16.9
Conventional (n^+p)	0.028	0.590	0.817	14.5
	50 suns			
	J_{sc}, A/cm^2	V_{oc}, V	FF	η, %
High-low junction emitter (n^+np)	1.69	0.792	0.842	24.4
Conventional (n^+p)	1.40	0.717	0.815	17.7

n layer are about equal and electrons and holes supporting the recombination currents from the base and emitter, respectively, must both drift across the n layer. This fact fixes the emitter recombination current at about μ_p/μ_n (about 1/3 in Si) times the base recombination current. Thus the hole current injected into the n^+region can be 30 times less than it is in the conventional structure. This results in a higher V_{oc}. Besides, a deeper pn junction can collect carriers more efficiently than a shallow junction, provided that the effective recombination velocity at the front surface is low; the n^+n junction does provide a low effective recombination velocity (see high-low junction in Sec. 3.8). The performances of a high-low junction emitter cell and a conventional cell as calculated with a simulation program (Sah, 1978) are shown in Table 11.1.

Graded-Bandgap Solar Cells

There are no physical reasons that make these cells more suitable for operation under concentrated sunlight than without concentration. Their high costs do make them less attractive for use without concentration. Some thin-film cells, however, offer the possibility of inexpensive graded-gap solar cells. The bandgap of amorphous silicon, for example, can be varied over a wide range by simply changing the film deposition conditions (Sec. 10.2).

Extending the concept of band diagram discussed in Sec. 3.2, it can be shown that a gradient in valence-band energy E_v is equivalent to an electric

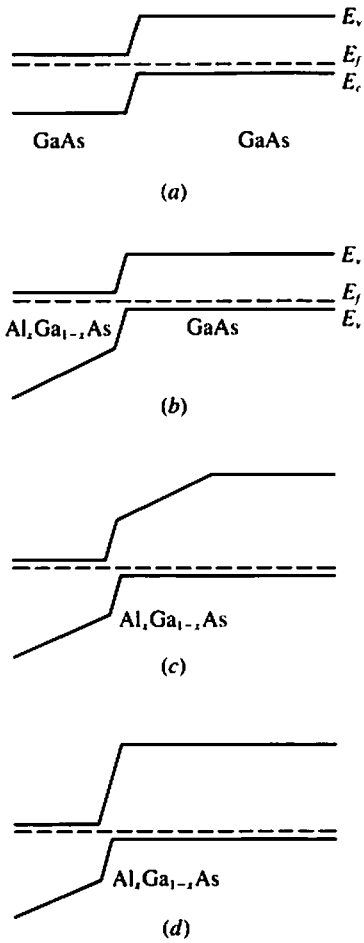

Figure 11.7 (*a*) The band diagram of the *pn* junction of a conventional GaAs cell. (*b*) The built-in drift field in a graded bandgap cell aids the collection of light-generated holes and increases J_{sc}. (*c*) When the drift field is built into both sides of the junction, the saturation current I_0 could be greatly reduced and V_{oc} increased. (*d*) This structure also can result in low I_0 and high V_{oc}.

field so far as holes are concerned. A strong drift field then can be built into a solar cell by grading the composition of a compound semiconductor and thus grading the bandgap as illustrated in Fig. 11.7*b*. AlAs and GaAs are completely miscible such that an alloy semiconductor $Al_xGa_{1-x}As$ can be formed with any x between 0 and 1. For $x < 0.34$, the bandgap E_g is a linear function of x. The resultant electric field in the graded-composition $Al_xGa_{1-x}As$ layer drives holes toward the junction and thus increases the collection efficiency. Computer analysis of the structure shown in Fig. 11.7*b* (Sutherland, 1977) predicts an efficiency of about 20 percent. This is not higher than the efficiency that can be expected from the conventional GaAs

cell with proper surface passivation, as mentioned in Chap. 4 and shown in Fig. 11.7*a*, because the collection efficiency of the conventional cell is already very high.

Graded-bandgap structures probably can be much more rewarding if their low saturation current, I_0, is exploited. The structure in Fig. 11.7*c* can have small I_0 because the built-in fields work against hole injection into the n side (left-hand side) and electron injection into the p side. In Fig. 11.7*d*, hole injection into the n side is reduced by the field and the electron injection into the p side is naturally low because of the large E_g of this p-type material (see Chap. 3). Ideally, I_0 and hence V_{oc} of both structures shown in Fig. 11.7*c* and *d* could approach that corresponding to the wide bandgap material and I_{sc} could approach that corresponding to the smallest E_g in the structure. In this way efficiencies higher than those possible with any single-material cell might be achieved (see Fig. 3.18).

Cascade Cell

Another multi-bandgap cell that can have higher efficiency than any single-material cell, the cascade cell, will be described in Sec. 12.2.

11.4 SUMMARY

Besides the more common *pn*-homojunction cells, the heterojunction cells, and the Shottky-junction cells, many unconventional cell structures have been investigated in recent years; a number of them are reviewed in this chapter. Most of the structural variations described here were proposed for improving cell performance.

Many unconventional concentrator cell structures address the series resistance loss problem. These include the parallel and series connected vertical junction cells and the back-contact cells. They may be useful for operation at 100× or higher concentrations. The high-low junction emitter cell and the graded-gap cell offer possibilities of higher cell current, voltage, and efficiency.

It may be more difficult to justify the higher costs of the unconventional cell structures on the basis of improved efficiencies for nonconcentrator cells than for concentrator cells (see Chap. 5). A few unconventional nonconcentrator cell structures, however, can potentially be the basis for low-cost solar cells. For example, the semiconductor/electrolyte junction cells are potentially inexpensive. The metal-insulator-semiconductor cell structure may be more suitable for use with low-cost polycrystalline cells than the *pn*-junction cell structure.

REFERENCES

Call, R. L. (1973), Final Report, JPL Contract 953461.
Card, H. C., and Yang, E. S. (1976), *Appl. Phys. Lett.*, Vol. 29, 51.
Chappell, T. I. (1978), Record, 14th IEEE Photovoltaic Spec. Conf., 791.
Electronics (1981), McGraw-Hill, 46, 24 February.
Frank, R. I., Goodrich, J. L., and Kaplow, R. (1980), Record, 14th IEEE Photovoltaic Spec. Conf., 423.
Green, M. A. (1975), *Applied Phys. Lett.*, Vol. 27, 287.
Hu, C., and Edleberg, J. (1977), *Solid State Elec.*, Vol. 20, 119.
Kim, Y. S., Drowley, C. I., and Hu, C. (1980), Record, 14th IEEE Photovoltaic Spec. Conf., 596.
Loferski, J. J., et al. (1972), Record, 9th IEEE Photovoltaic Spec. Conf., 19.
Muller, J. (1978), *IEEE Trans. Elec. Dev.*, Vol. ED-25, 247.
Sah, C. T., Lindholm, F. A., and Fossum, J. G. (1978), *IEEE Trans. Elec. Dev.*, Vol. 25, 66.
Sater, B. L., and Goradia, C. (1975), Record, 12th IEEE Photovoltaic Spec. Conf., 356.
Schwartz, R. J., and Lammert, M. D. (1975), Internat'l Elec. Devices Conf., 350.
Shewchun, J., Burk, D., and Spitzer, M. B. (1980), *IEEE Trans. Elec. Dev.*, Vol. 27, 705.
Sutherland, J. E., and Hauser, J. R. (1977), *IEEE Trans. Elec. Dev.*, Vol. 24, 363.

PROBLEMS

11.1 *Classification of unconventional cells* In this chapter, the unconventional cell structures are divided, sometimes rather arbitrarily, into concentrator and non-concentrator cells. Try, instead, to classify them as structures that (*a*) reduce costs, (*b*) reduce the series resistance effect, (*c*) improve J_{sc}, (*d*) improve V_{oc}. One structure may fall into more than one category.

11.2 *Examine a cell in depth* Select one unconventional structure described in this chapter and discuss its advantages and disadvantages in some detail.

11.3 *Invent a solar cell* You may have thought of a new variation in cell structures. (It may be a small modification to one of the structures discussed in this chapter.) Describe it and discuss its advantages and disadvantages.

CHAPTER

TWELVE

UNCONVENTIONAL CELL SYSTEMS

CHAPTER OUTLINE

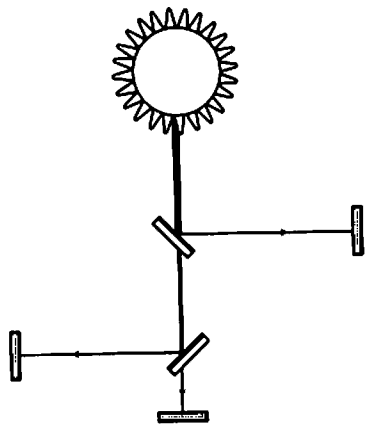

Four unconventional cell systems are described in this chapter. The first system employs a combination of individual cells, each optimized to convert the energy in a narrow spectrum of sunlight. Efficiencies higher than 30 percent are certainly within reach and 40 percent may be possible. This concept may be implemented with spectrum splitting or cascade cells.

The second system also exploits the fact that a solar cell can be very efficient in converting energy in a narrow spectrum. Called *thermophotovoltaic* conversion, sunlight is concentrated in this system to heat a refractory metal "radiator" to a very high temperature. A silicon cell then converts the blackbody radiation from the radiator into electricity. The radiation below the Si bandgap energy is reflected back to the radiator to keep it hot.

The third system does not strive for unusually high efficiency. Rather, it generates hydrogen instead of electricity as the end product. One potential advantage of such a system is that hydrogen can be stored more economically than electricity.

A fourth system puts the solar cell panel in a geosynchronous space orbit and beams power to earth via microwaves. The solar insolation in space is about five times higher than on earth and is unaffected by weather or day-night cycles. Thus this system has the unique ability to provide reliable, base-load power.

12.1 MULTIPLE-CELL SYSTEMS: SPECTRUM SPLITTING AND CASCADE CELLS

It was pointed out in Chap. 3 (Fig. 3.17) that the combined lost energy due to photon energy in excess of bandgap and energy of photons incapable of generating charge carriers account for over half of the energy entering a conventional solar cell. The loss due to excess photon energy may be reduced by increasing the bandgap E_g, but the loss due to photons incapable of generating carriers will also rise as a result. These losses would be markedly smaller if the spectrum of the light were narrower.

To take advantage of this fact, the sunlight spectrum may be split into parts with each part directed to a separate cell designed to operate efficiently for that part of the spectrum. Physically, the solar spectrum may be split with special filters, as shown in Fig. 12.1*a*. Each filter reflects a portion of the solar spectrum and transmits the rest.

An alternative arrangement is shown in Fig. 12.1*b* where cell 1 material has a wider bandgap than cell 2 material, and so on. Compared to Fig. 12.1*a*, the tandem cell scheme does not require the filter/mirrors but places more stringent requirements on the minimization of shadowing by the front and

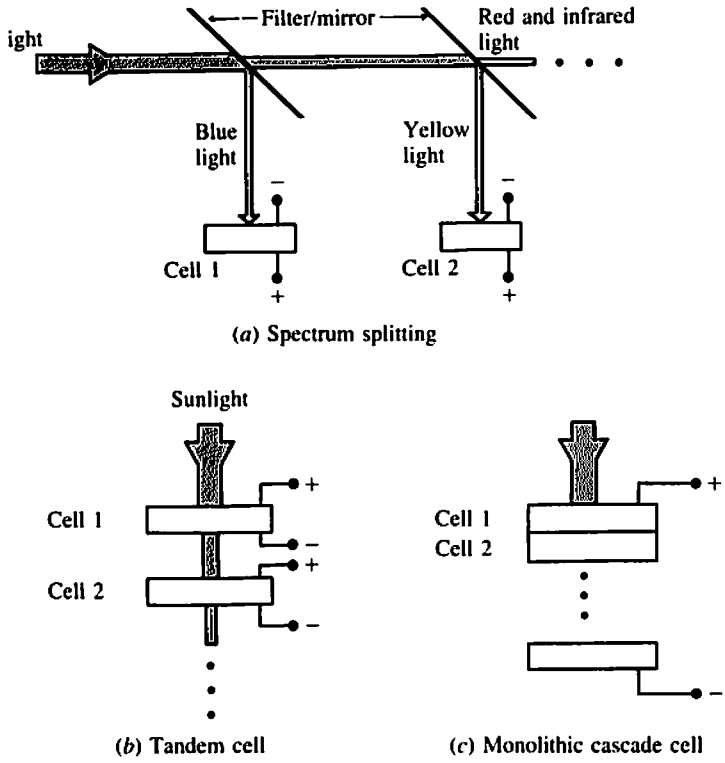

Figure 12.1 Systems employing multiple cells, each optimized for a narrow spectrum of sunlight, can have far higher efficiencies than single-cell systems. (*a*) The sunlight spectrum is split into narrow bands with wavelength-dependent filter/mirrors. (*b*) The cells double as wavelength-dependent filters. Cell 1 material has wider bandgap than cell 2 material and so on. (*c*) Similar to (*b*). In addition, cells are electrically connected in series and mechanically integrated into a single piece.

back contacts and of spurious absorption and reflection in each cell. The principle of operation, however, is the same.

Bennett (1978) has calculated the efficiencies of these two schemes and the results are shown in Fig. 12.2. The ideal system curve assumes zero contact shadowing and cell reflectance and perfect filter/mirrors. The spectrum splitting curve assumes 5 percent reflectance loss, 5 percent transmission loss at the filter/mirrors, and 5 percent shadowing and reflection losses at the cells. The tandem cell curve assumes 5 percent shadowing and reflection loss and 90 percent cell transmittance. It appears that there is little incentive to use more than two or three cells. A two-cell system should consist of cells made from 1.0- and 1.8-eV bandgap materials; and a three-cell system, 1.0-, 1.6-, and 2.2-eV bandgap materials.

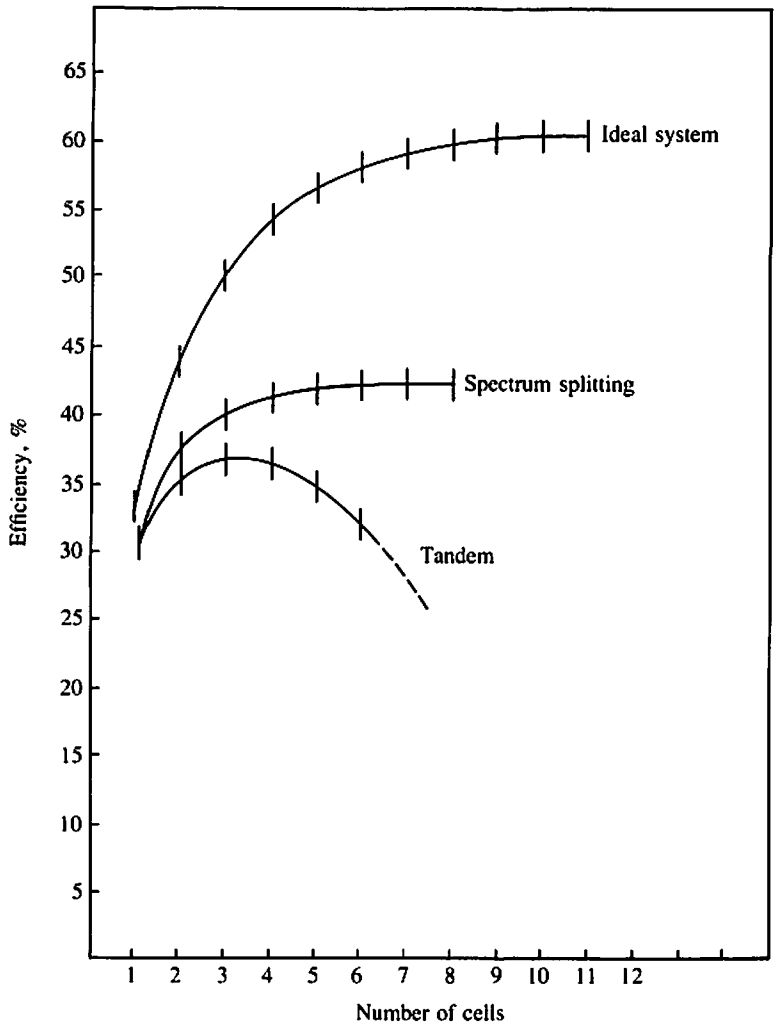

Figure 12.2 Calculated efficiency of multiple cell systems. The spectrum-splitting curve assumed 5 percent reflectance loss and 5 percent transmission loss at each filter/mirror. The tandem cell curve assumes 5 percent contact shadowing and reflection loss, and 90 percent transmittance at each cell, 1000× AM1 sun. (*Bennett, 1978.*)

A more thorough analysis of the two-cell system was made by Masden (1978), whose results are shown in Fig. 12.3. The calculated efficiency at 100× solar concentration is plotted as a function of the two bandgap energies, E_{g1} and E_{g2}. The optimum combination is 0.95 eV and 1.75 eV, which results in an efficiency of 42 percent. This is a higher efficiency than indicated in Fig.

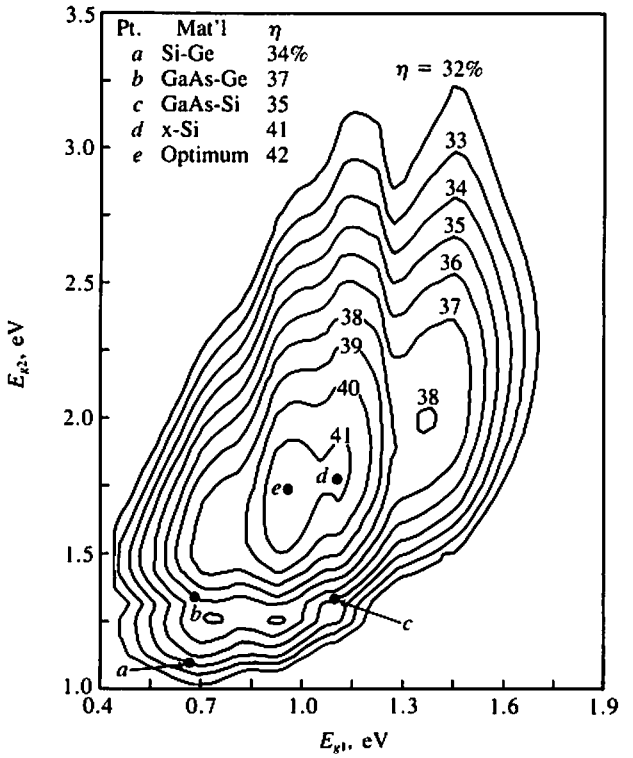

Figure 12.3 Limit conversion efficiency contours for two-cell spectrum-splitting systems for AM2 and 100× concentration. (*Masden, 1978.*)

12.2 for a two-cell system. The difference is due to the different cell efficiency models used. Several promising near-term candidates are also highlighted in Fig. 12.3. Both the GaAs/Si system and the Si/Ge system yield about 34 percent.

The measured efficiency of a Si/AlGaAs two-cell system using one filter/mirror was 28.5 percent at 165× concentration (Moon, 1978). In that experiment, the Si cell alone contributed 11.1 percent to the efficiency and the AlGaAs cell contributed 17.4 percent. The same Si cell operating under full solar spectrum yielded about 15 percent efficiency and the AlGaAs cell (1.6-eV bandgap), 20 percent. The filter/mirror used was a 17-layer dielectric filter of alternating ZnS and Na_3AlF_6.

Both the configurations shown in Fig. 12.1*a* and *b* can be operated in an alternative mode, with all cells connected in series. This mode of operation would simplify the electrical connections but would significantly reduce the system efficiency and limit the choice of cell materials. In a series connection, all cells should provide identical short-circuit currents, otherwise the output

current of the system will be limited by the cell with the least current, as is the case with all series-connected cell systems.

Figure 12.1*c* shows a particularly attractive arrangement of series-connected cells. The design is a monolithic version of the tandem cell configuration (with internal series connection). The cells are likely made in epitaxial materials grown layer upon layer. The amount of semiconductor used is much less than in Fig. 12.1*b* and the transmittance of each cell is probably higher. The electrical connection between cells could be the ohmic contact between p^+ and n^+ semiconductors. For example all cells may have n^+pp^+ structures. The p^+ layer of the first and the n^+ layer of the second cell form a low-resistance ohmic junction sometimes called a *tunnel* junction. Making heavily doped layers and low-resistance junctions in wide-gap semiconductors, however, is not a simple task.

In the cascade cell, a requirement for high efficiency is that each cell produce the same short-circuit current. If one assumes an internal collection efficiency, the number of cells, and the bandgap of the bottom cell in the stack, then the bandgaps of the other cells can be determined from the requirements of equal photon flux within the spectrum absorbed by each cell. These combinations of bandgaps and the resultant efficiencies are shown in Fig. 12.4. The efficiencies are lower than those shown in Figs. 12.2 and 12.3 because the series-connected cells must satisfy the added condition of equal current from each of the sub-cells.

In designing a monolithic cascade cell one must not only consider the bandgaps of the materials in the system but also their lattice constants. High-quality epitaxial materials can only be grown on substrates of closely matched lattice constants. Figure 12.5, for example, helps determine the suitable materials for a two-cell or two-junction cascade cell. Each point represents the E_g and lattice constant of a candidate material. Each curve represents the continuous range of possibilities obtainable by mixing the materials at the two ends of the curve in varying proportions. The curve connecting GaAs and AlAs, for example, represents the E_g and lattice constant of $Al_xGa_{1-x}As$. The two bands of shaded regions represent the desired bandgaps of the two cells. These bandgaps are larger than one would deduce from Fig. 12.4, because the authors of Fig. 12.5 (Bedair et al., 1980) assumed a higher operating temperature range. The objective is to find one material from each band such that the two have closely matched lattice constants (within 0.1 Å).

Several other materials problems need consideration. The thermal expansion coefficients should be matched so that the lattice constants match at the material growth temperature as well as at room temperature. The substrate should ideally be inexpensive and readily available—Si, GaAs, Ge, InP, InAs, and GaSb in descending order of preference. Finally, the maturity of

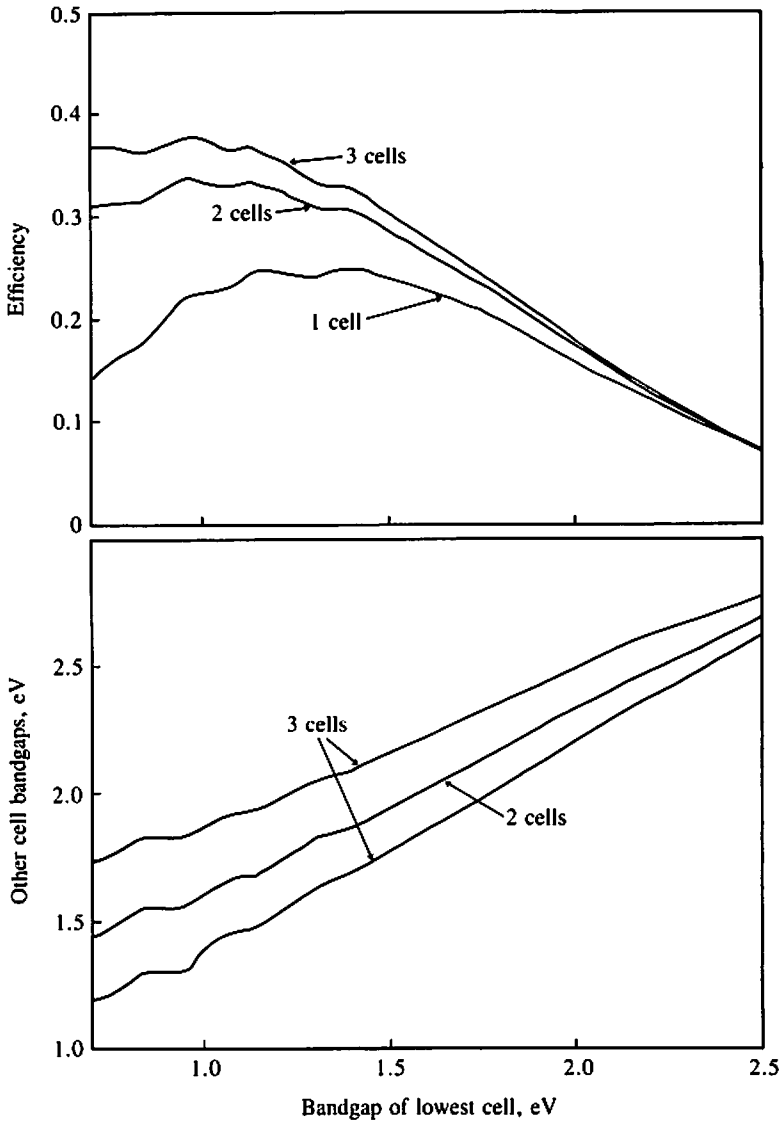

Figure 12.4 Efficiency and bandgaps of two or three cells electrically connected in series. 1000× AM2 sun, 30°C, and 80 percent collection efficiency. (*Moon, 1978.*)

the processing technology for the chosen materials is an important consideration for near-term development work. So far only experiments with GaAs/AlGaAs (Bedair et al., 1980), GaAs/GaAsP (Fraas et al., 1982), and amorphous silicon (p. 210) have been reported.

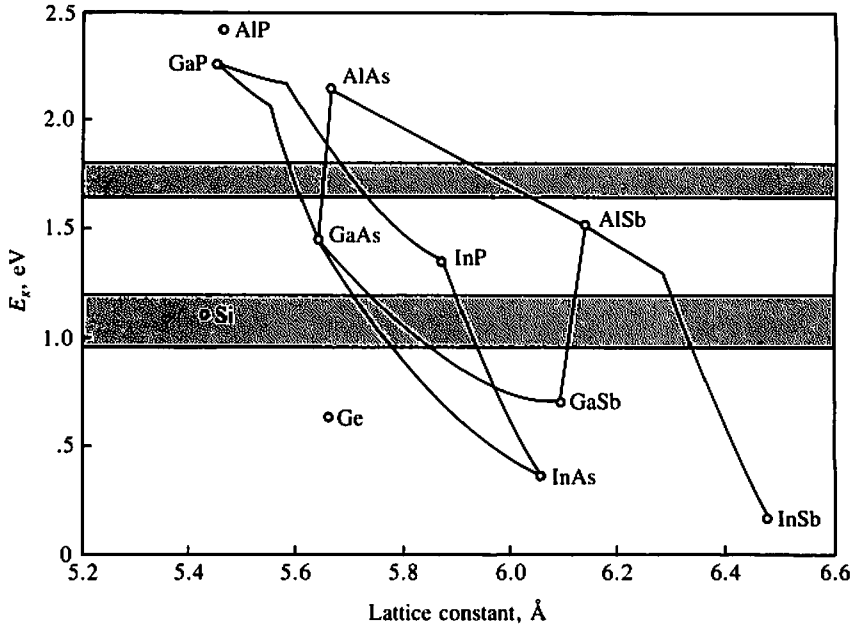

Figure 12.5 Lattice constants and bandgaps of some candidate materials for two-cell monolithic cascade cells. (*Bedair, 1980.*)

12.2 THERMOPHOTOVOLTAIC (TPV) SYSTEM

A thermophotovoltaic system generates electricity by photovoltaic conversion of radiation from an adjacent radiating surface (Wedlock, 1963). In a solar-powered thermophotovoltaic converter a parabolic mirror concentrates sunlight into a secondary concentrator (Fig. 12.6*a*) and finally on a refractory radiator (Swanson, 1979). The concentration ratio is several thousand so that the radiator can be heated to over 2000 K. The reason for the high temperature is that the cell efficiency is lower at lower temperatures, as shown in Fig. 12.7.

Both the unusually high efficiency and its strong temperature dependence can be explained with the diagram in Fig. 12.8. In a conventional Si cell, half of the energy is lost due to photon energy in excess of the bandgap and photons that are not absorbed. In the thermophotovoltaic system, loss of photon energy in excess of bandgap is minimized because the blackbody radiation flux decreases rapidly at energies about 1.1 eV, in accordance with Planck's law. The photons below the bandgap can be reflected from the back surface of the cell toward the radiator. If there were no parasitic absorption of these below-bandgap photons, their energies simply could not be lost. These, then, are the reasons for the high efficiency.

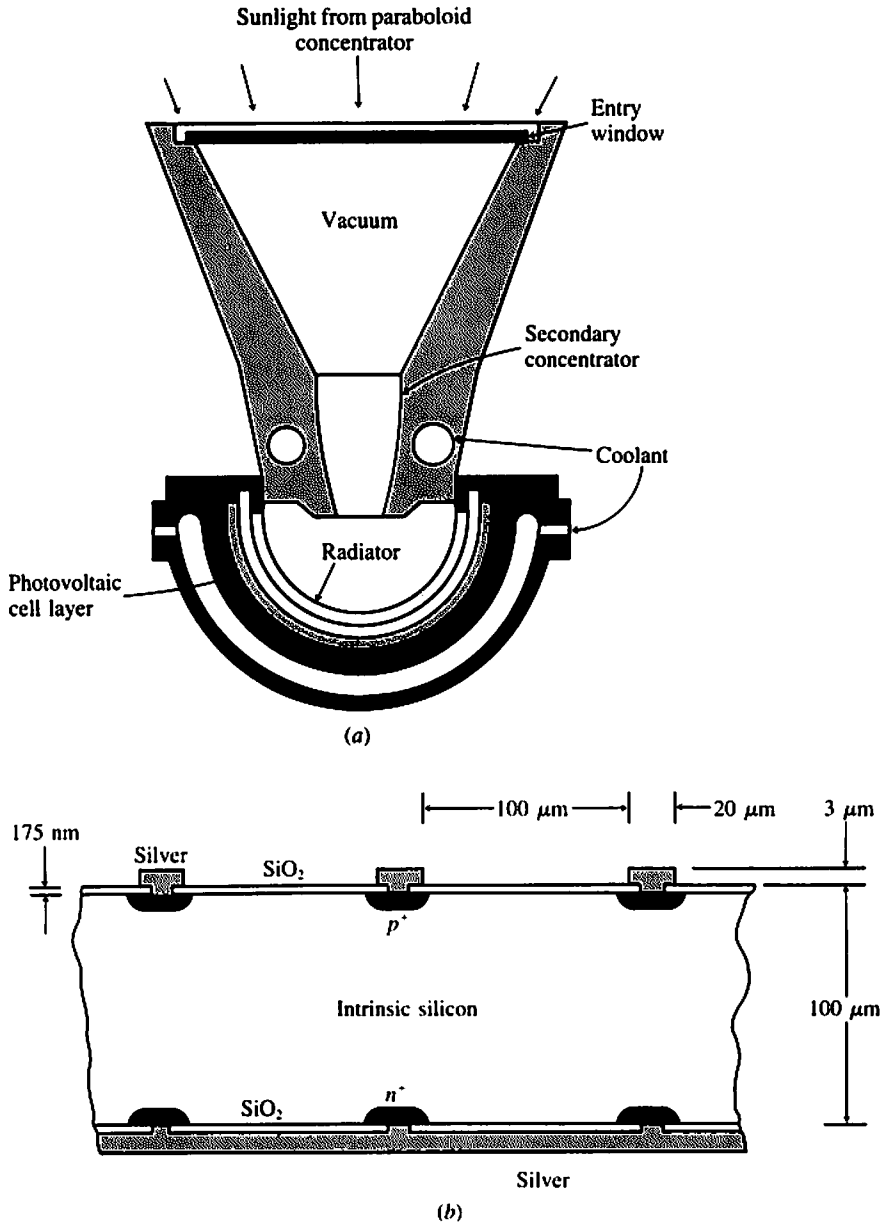

Figure 12.6 (*a*) Secondary concentrator of a thermophotovoltaic (TPV) system. (*b*) One cell structure developed for the TPV system. (*Swanson, 1979.*)

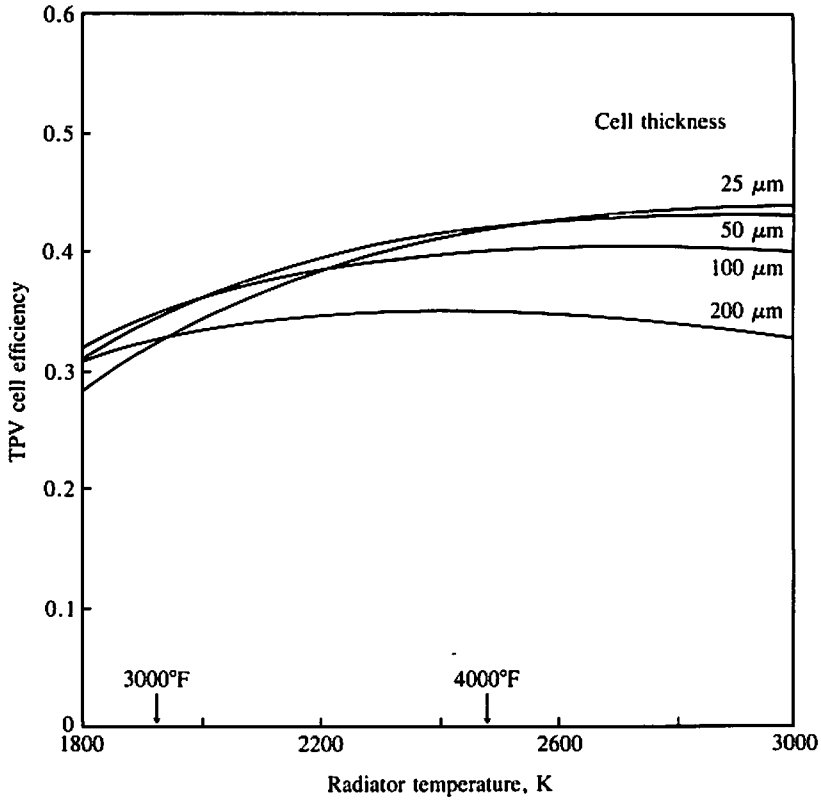

Figure 12.7 Calculated cell efficiency of a TPV cell. *(Swanson, 1979.)*

The need for high radiator temperature is explained as follows. Even at 2000 K, only 10 percent of the blackbody radiation is above the 1.1-eV photon energy. If a small percentage of the remaining 90 percent of the radiation is absorbed by the cell, the cell efficiency is significantly reduced. This becomes more serious at low radiator temperatures, at which an even smaller portion of the radiation is above the 1.1-eV photon energy.

It should be clear by now that the main task of *cell* development is to reduce the absorption of below-bandgap photons. The cell shown in Fig. 12.6*b* has been developed for this system. Using an electrically heated tungsten radiator, 29 percent conversion efficiency has been measured. This efficiency, although very high, is still below the projected 40 percent shown in Fig. 12.7 because of higher parasitic absorptions than assumed. There has been no report of solar energy conversion efficiency using this concept.

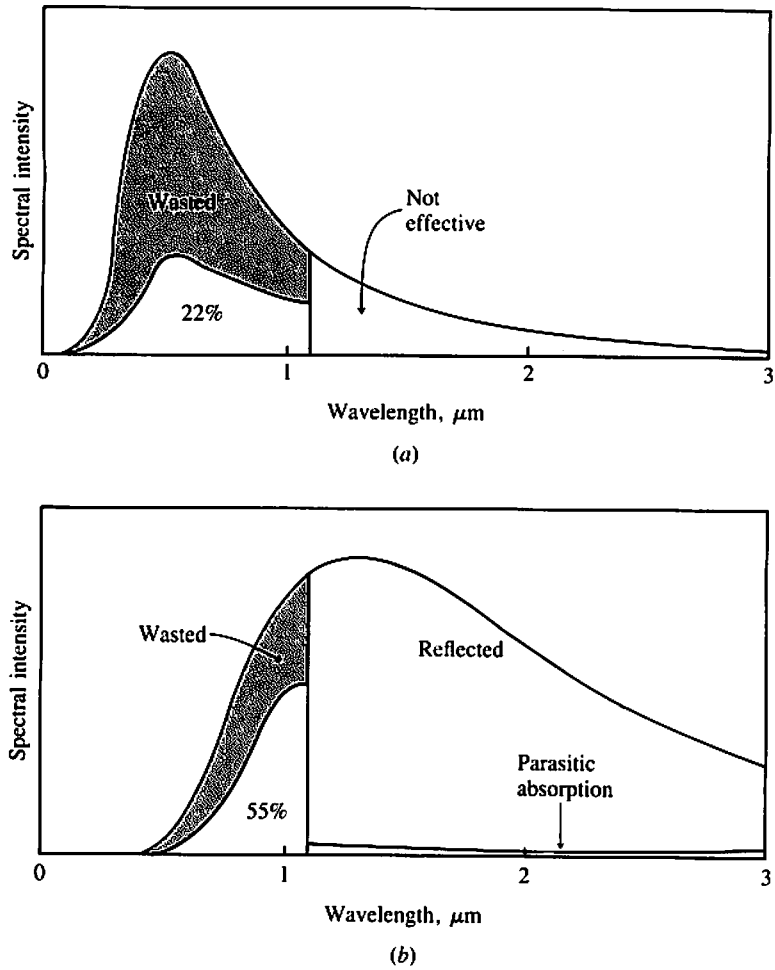

Figure 12.8 Comparison between the energy losses of (*a*) a conventional solar cell and (*b*) a TPV cell. *(Swanson, 1979.)*

12.3 PHOTOELECTROLYTIC CELL

A photoelectrolytic cell employs photovoltaic cells or photochemical processes to decompose water into H_2 and O_2. The hydrogen can be stored, burned as fuel, or used in a fuel cell to produce electrical energy. The energy conversion is from sunlight to chemical energy. The decomposition of water

is the most attractive reaction, but the chemical energy may also be stored in other forms.

The photoelectrolytic cell should be distinguished from the electrochemical photovoltaic cell such as the liquid junction cell discussed in Chap. 11. An electrochemical photovoltaic cell produces electricity, and steady-state chemical reactions are to be avoided. Yet a third type of electrochemical cell is the *photogalvanic* cell, in which the incident light is absorbed by molecular species in the solution and electrical power is generated by charge transfer from excited molecular species to electrodes—a rather inefficient process. Only the photoelectrolytic cell will be discussed here.

There are two categories of photoelectrolytic cells. The first may be called the *photovoltaic-electrolysis* cell and is basically a variation of a photovoltaic cell driving a conventional electrolysis cell, as shown in Fig. 12.9*a*. When a sufficient voltage is applied between the electrodes of the electrolysis cell, current begins to flow and hydrogen and oxygen evolve at the cathode and the anode, respectively. The free energy change for the conversion of liquid water to H_2 demands a minimum voltage of 1.23 V. Depending on the electrode material, an "over-voltage" is also required. Platinum is the most popular electrode material because of its chemical stability and negligible over-voltage. The electrolyte also presents an ohmic drop.

Figure 12.9*b* shows a way of integrating the photovoltaic cell and the electrolytic cell. The photovoltaic cell may consist of two Si cells in series in order to obtain sufficient voltage. Both surfaces are coated with thin transparent Pt films and the edges are insulated from the electrolyte. Notice that no external wiring is needed.

A development (Kilby, 1979) from Texas Instruments has caused considerable excitement. It includes a potentially inexpensive way of making the photovoltaic cells used in Fig. 12.9*b*. A schematic of the finished photovoltaic cell is shown in Fig. 12.9*c*. The spheres are silicon. They are made with a process similar to that used for making lead shot. Silicon doped to 5×10^{17} cm^{-3} is melted in a tube and forced through a nozzle. Silicon droplets are formed and permitted to fall a distance of about 8 ft. During this fall the silicon solidifies. Both *p*-type and *n*-type spheres are prepared in this manner. Although some of the spheres may have internal grain boundaries, most will be suitable for solar cell application. The spheres may then be sorted by diameter into groups within 0.001-inch diameter variation.

Figure 12.9 (*a*) A photovoltaic cell powering an electrolysis cell. (*b*) The wiring in (*a*) is eliminated by immersing the photovoltaic cell in the electrolyte. Two solar cells are connected in series through ohmic contacts to produce the necessary voltage. (*c*) This cell is identical to the solar cell shown in (*b*) in function, but may be produced inexpensively. (*d*) A proposed photoelectrolysis cell system. (*Kirby, 1979.*)

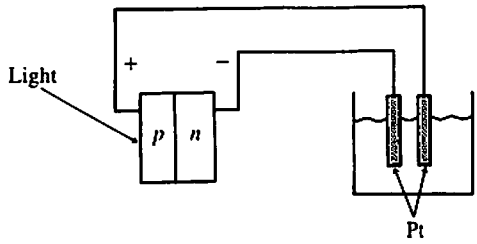
Light
+
−
p
n
Pt

(a)

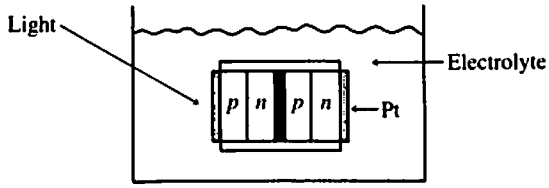
Light
Electrolyte
p
n
p
n
Pt

(b)

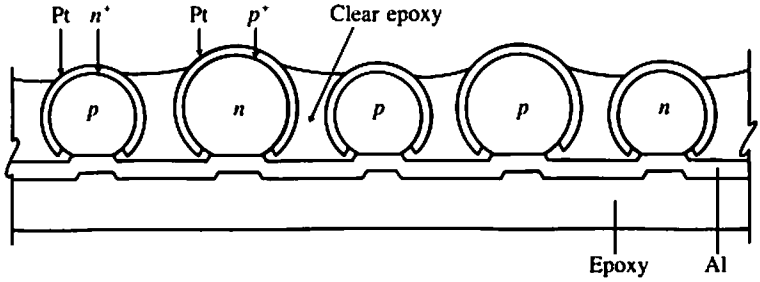
Pt
n+
Pt
p+
Clear epoxy
p
n
p
p
n
Epoxy
Al

(c)

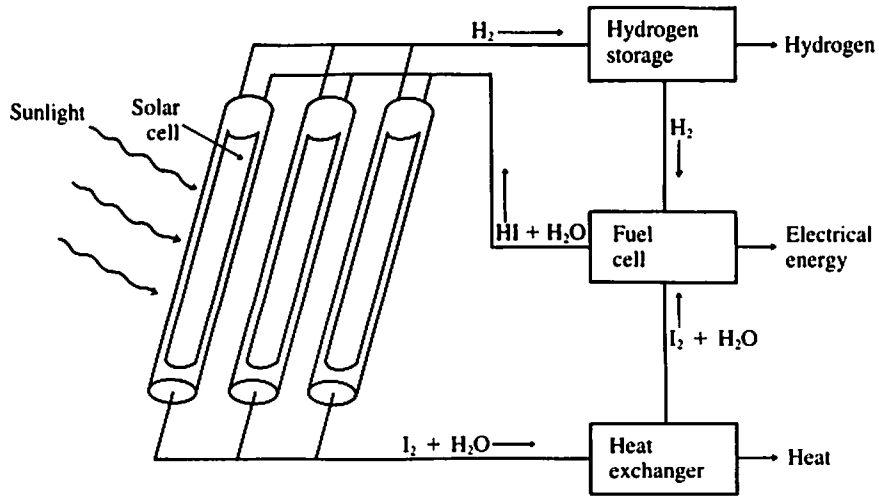
H2
Hydrogen storage
Hydrogen
Sunlight
Solar cell
H2
HI + H2O
Fuel cell
Electrical energy
I2 + H2O
I2 + H2O
Heat exchanger
Heat

(d)

The p-type spheres are given an n-type surface layer and the n-type spheres are given a p-type surface layer by diffusion. A 150-Å-thick Pt film is applied to the entire surfaces of the spheres by sputtering. Platinum forms ohmic contacts to both p-type and n-type silicon. Then a 0.0005-inch layer of insulating acrylic coating is applied.

The n-type and p-type spheres are now mixed and spread on a temporary substrate coated with a thin layer of wax. The substrate is heated and the spheres are partially pressed into the wax. By inverting Fig. 12.9*c* and imagining the surface of the clear epoxy as the surface of the wax, one can envision the steps just described. At this time the substrate and the spheres are flooded with a layer of clear silicone resin or epoxy. After curing, the top surface of the epoxy is lapped off to expose the cores of the spheres.

The n^+ and p^+ surface layers are etched back using a concentration dependent etch. After etching, the surface of the sheet is heated, causing the feather edges of silicone resin at the top surfaces of the spheres to sag over and protect the exposed junctions. A 50-μm-thick Al layer is then plated over the entire surface and a thick epoxy layer is applied for protection and mechanical strength. The lower portion of the sheet is now washed with a solvent to remove wax and expose the Pt. Upon turning the sheet upside down, the structure shown in Fig. 12.9*c* is obtained. *Electrical* efficiency of 13 percent has been reported for a similar sheet (Johnson, 1981).

This is a potentially inexpensive method of making large sheets of Si solar cells. Notice that the sheet consists of many n^+p and p^+n cell pairs connected in series by the Al film. Kilby proposed to use an aqueous solution of hydrogen iodide as the electrolyte in a system shown in Fig. 12.9*d*. Hydrogen may be stored in a metal hydride and used to generate electricity through a fuel cell (Johnson, 1981). The total efficiency from sunlight to electricity has been about 5%. Recent work aims at developing a 32 ft^2, 300 W_{pk} module having 1500 Wh storage and an overall system efficiency of 6% (McKee, 1982).

The second category is considered by some as the *true* photoelectrolytic cell. At first sight, Fig. 12.10*a* and 12.10*b* are the same as Fig. 12.9*a* and 12.9*b* with liquid junction photovoltaic cells. Photocatalysis and reactions involving intermediate states may occur at the semiconductor surfaces in Fig. 12.10*a* but not the Pt surfaces in Fig. 12.9*a*. Nozik (1977) also pointed out that the internal potential available for driving the cell reaction may be higher than the photovoltage of the liquid junction cell measured externally.

Photoelectrolytic cells of the configuration shown in Fig. 12.10*a*, using a wide-gap semiconductor such as TiO_2, are almost universally used for basic studies and demonstrations. The configuration shown in Fig. 12.10*b* can simplify the cell. It also illustrates the possibility of using two low-energy-gap semiconductors such as Si connected by an ohmic contact to drive photoelectrolysis. The efficiency limit of photoelectrolysis using Si has been esti-

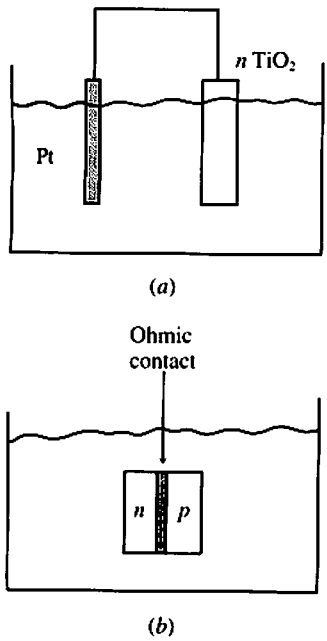

Figure 12.10 Photoelectrolysis cells in which the semiconductor/electrolyte interfaces play an active role.

mated to be about the same as Si photovoltaic cells, i.e., about 20 percent (Nozik, 1977).

12.4 SATELLITE POWER SYSTEM (SPS)

While the preceding unconventional photovoltaic systems strive to increase the energy conversion efficiency or to provide energy storage, the satellite power system would increase the solar radiation on the solar collector and eliminate the need for energy storage. In this proposed system (Figure 12.11), a satellite carrying a large solar cell panel in geosynchronous (also known as geostationary) orbit transmits power via a beam of microwaves to an antenna array on the earth's surface, where the microwaves are received and rectified into dc electricity. The advantage of placing the solar cells in space is that they will receive the full AM0 radiation more than 99 percent of the time, regardless of weather or the the day-night cycles of the earth. The solar insolation on the cells will be 32 $kWh/m^2 \cdot day$. For comparison the long-term average insolation at a desert location on earth is only about 6 $kWh/m^2 \cdot day$ without solar tracking and 7.5 $kWh/m^2 \cdot day$ with solar tracking.

This imaginative system was first suggested by Dr. Peter Glaser in 1968 and has been under study by the U.S. National Aeronautics and Space Ad-

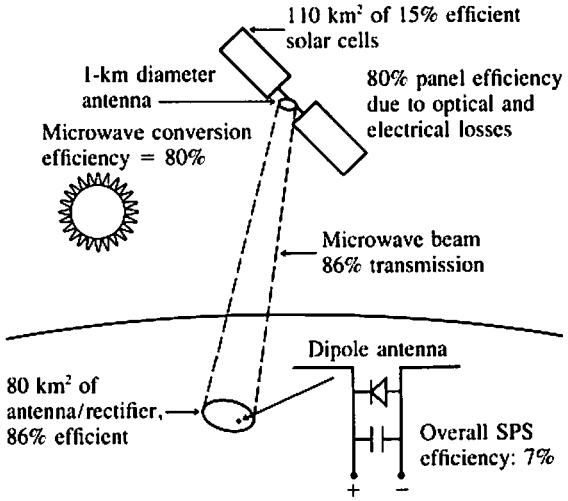

Figure 12.11 In the space power system, a satellite in geosynchronous orbit beams microwaves to earth, where the microwave is rectified into dc electricity. The numbers shown are for a proposed 10-GW system.

ministration (NASA) since 1972. Although there has been some evolution in the proposed designs of this system, the more recent conceptual designs (Brown, 1973; Glaser, 1977; DOE/NASA, 1978) differ from one another mostly in details. The following is a composite summary of these recent designs.

Each system will probably produce 10 GW (10,000 MW) of electricity on earth with an overall efficiency of about 7 percent (see Fig. 12.11). This means that the solar cell panel is about 110 km^2 in size. To save the cost of transporting materials, the SPS satellite can be built in a low earth orbit, and once completed, would itself supply power to a bank of ion thrustors. These thrustors, operating for a period of several months, would propel the satellite into a geosynchronous orbit 35,700 km above the equator. In this orbit, the satellite is stationary relative to the earth. In the earth-centered view of the sun-earth system in Fig. 2.1*b*, the SPS satellite would be located at a fixed point in the equatorial plane and separated from the earth by about three earth diameters. Obviously, the solar panel has to rotate once a day in order to track the sun (while the microwave antenna points at the earth all the time). The solar panel receives full AM0 radiation except when eclipsed by the earth's shadow. These eclipses occur once a day for 22 days before and after vernal and autumnal equinoxes (March 22 and September 23). These eclipses, which always occur around midnight, last no longer than 1 hour and 12 minutes, resulting in a yearly average duty cycle of over 99 percent.

Silicon solar cells operating without solar concentration at 15 percent efficiency are commonly assumed in SPS designs. The exact cell material and configuration will be determined by the usual cost and efficiency considerations and the added requirements of light weight and resistance to radiation of high-energy particles. The dc electricity is converted to 2.45-GHz (12-cm wavelength) microwaves with several million vacuum-tube-type oscillators and amplifiers. This frequency is chosen because lower frequencies would require the use of larger antennae and higher frequencies would increase the energy losses in the microwave amplifiers and raise the transmission loss in the atmosphere. The transmitting antenna has a diameter of 1 km and must generate a wavefront that is flat to one-quarter wavelength (3 cm) through tight mechanical tolerance and/or electronic control of the phases of subsegments of the antenna. The antenna must maintain a pointing accuracy measured in arc seconds and directed at a receiving antenna-array on the earth. The receiving antenna-array covers an area about 10 km in diameter and consists of a large number of dipole antenna elements, each feeding microwave power to a separate GaAs rectifier, where the power is converted efficiently into dc electricity. Because the rectifiers are small, probably several hundred million dipole elements and rectifiers will be required. The dc electricity can then be interfaced with the utility grid through an inverter.

Glaser (1977) has put the estimated system cost at \$1500/kW (in 1974 dollars). According to this estimate (Fig. 12.12), the solar cell array accounts for only 25 percent of the system cost. This same array, if installed on earth, would generate 40 percent ($6\ \text{kWh/m}^2 \cdot \text{day} \cdot 15\% \div 32\ \text{kWh/m}^2 \cdot \text{day} \div 7\%$) of the SPS output. If no credit is given to energy storage, it seems that SPS would be less cost-effective than a ground-based system, according to this rough comparison. Further reduction in solar cell cost will tip the comparison more in favor of a ground-based system. Figure 12.12 shows that the largest cost item is space transportation. More recent designs (DOE/NASA, 1978)

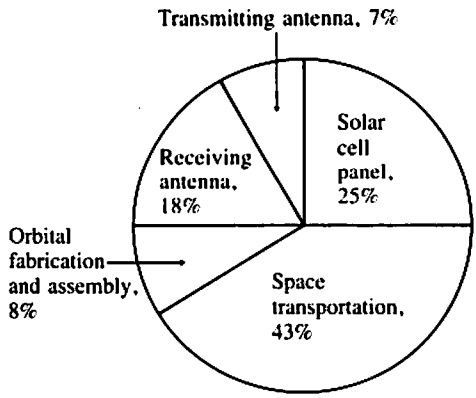

Figure 12.12 Breakdown of the estimated cost of a proposed SPS (*Glaser, 1977*). The estimated cost is \$1500/kW in 1974 dollars.

placed the estimated weight of the satellite (77×10^6 kg) at over twice the estimate of Glaser (1977) making the share of the space-transportation cost even larger than that shown in Fig. 12.12. This, too, would make the comparison more favorable for a land-based system. In any event, the coming of SPS must await the successful development of low-cost space transportation technology and the technology of building large structures in space. Many people are also disturbed by the potential health hazard posed by the powerful microwave system. The intensity of the microwave beam is about 23 mW/cm^2 at the center of the receiving antenna field, gradually dropping toward the edge of the field. At the outside edge of the buffer zone surrounding the antenna field, the microwave intensity is 0.1 mW/cm^2, which is 100 times lower than the current U.S. exposure standard (10 mW/cm^2), but still ten times higher than the Soviet occupational standard of 0.01 mW/cm^2.

The Glaser (1977) article prompted about a dozen critical letters from the readers of *Physics Today*. Besides pointing to the economic, technical, and safety problems of SPS, some readers opposed the diversion of development effort from smaller, land-based photovoltaic systems. White (1977) pointed out that "Dispersed land-based converters would offer unique hope for the two million villages of the less-developed countries to maintain their individual characteristics and yet enjoy improved living conditions resulting from the availability of modest amounts of electric power obtained locally. . . ." Karr (1977) saw the size and complexity of SPS as trademarks of a military-aerospace complex and proclaimed, "I see no reason why a few unproductive aerospace corporations should be allowed to own the sun."

12.5 SUMMARY

Both the multiple-cell system and the thermophotovoltaic system avoid the inability of any single conventional solar cell to convert light in the broad solar spectrum efficiently. The multiple-cell system employs two or more solar cells each optimized to convert light in a narrow segment of the solar spectrum efficiently. The thermophotovoltaic system first shifts the spectrum to lower energies and then "recycles" the below-bandgap photons.

Both systems promise efficiencies in excess of 30 percent. They offer insights into some of the limitations of conventional solar cells and demonstrate the possibility of achieving significantly higher efficiencies than possible with the conventional cells.

The photoelectrolytic cell system eases the energy-storage problem by generating hydrogen. The photoelectrolytic cell can potentially be produced inexpensively, as demonstrated by one example.

The satellite power system has the unique advantage of providing base-

load power. It is an intriguing option for the future but will probably not become economically competitive with land-based photovoltaic systems for a long time.

REFERENCES

Bedair, S. M., Phatak, S. B., and Hauser, J. R. (1980), *IEEE Trans. Elec. Dev.*, Vol. 27, 822.
Bennett, A., and Olsen, L. C. (1978), Record, 13th IEEE Photovoltaic Spec. Conf., 868.
Brown, W. C. (1973), *IEEE Spectrum*, March, 38.
DOE/NASA (1978), Reports from the Satellite Power System Concept Development and Evaluation Program, Report HCP/R-4024.
Fraas, L. M., Sawyer, D. E., Cape, J. A., and Shin, B. (1982), Record 16th IEEE Photovoltaic Spec. Conf. (to be published).
Glaser, P. E. (1977), *Physics Today*, February, 30.
Johnson, E. L. (1981), Tech. Digest of IEEE Internat'l Electron Devices Meeting, 2.
Karr, T. (1977), *Physics Today*, July, 12.
Kilby, J. S., Lathrop, J. W., Wilbur, S. C., and Porter, A. (1979), U.S. Patent 4, 136, 436.
Masden, G. W., and Backus, C. E. (1978), Record, 13th IEEE Photovoltaic Spec. Conf., 853.
McKee, W. R., Carlson, K. R., and Levine, J. P. (1982), Record 16th IEEE Photovoltaie Spec. Conf. (to be published).
Moon, R. L., et al. (1978), Record, 13th IEEE Photovoltaic Spec. Conf., 859.
Nozik, A. J. (1977), Semiconductor Liquid-Junction Solar Cells, A. Heller, ed., Electrochemical Society, Inc., Princeton, New Jersey.
Swanson, R. M. (1979), Project Report ER-1271, EPRI, Palo Alto, Calif.
Wedlock, B. D. (1963), Proc. IEEE, Vol. 51, 694.
White, R. M. (1977), *Physics Today*, July, 11.

PROBLEMS

12.1 *A simple question* Why do Figs. 12.1, 12.2, and 12.3 all assume sunlight concentration?

12.2 *Match materials* Considering only the issues of lattice constants and bandgap energy, which materials in Fig. 12.5 best meet the requirements? If Si must be one of the materials used, which material should be chosen as the second material?

12.3 *Improve the thermophotovoltaic cell* The lower illustration in Fig. 12.8 shows the spectral intensity $I(\lambda)$ of blackbody radiation. The spectral intensity of radiation from any real emitter would be $I(\lambda) \cdot \epsilon(\lambda)$, where $\epsilon(\lambda)$, the emissivity of the radiator, may be a function of λ and has values between 0 and 1. Draw a desirable ϵ vs. λ relationship, and explain your drawing.

12.4 *Efficiency and power density of TPV* The total blackbody radiation intensity is $5.67 \times 10^{-8} \cdot T^4$ W/m$^2 \cdot$ K^4, where T is the radiator temperature in degrees Kelvin. Assume $T = 2000$ K and that 10 percent of the total radiation is above the bandgap energy and 90 percent is below the bandgap energy. Also assume that the photovoltaic cell converts the above-the-bandgap photons into electricity at 50 percent efficiency and absorbs 5 percent of the below-the-bandgap radiation. What is the radiation-to-electricity conversion efficiency? What is the electric power output per square centimeter of cell area? Someone has suggested heating the radiator by burning fuel and using the fuel-powered TPV converter to drive an electric car. Would the cell/radiator area required for a 20-kW-TPV converter be practical for a passenger car?

12.5 *Another spectrum shifting idea* Certain phosphors can absorb two photons of lower energies and re-emit one photon of a higher energy. How would you make use of such phosphors to improve the efficiency of Si solar cells? What are the potential problems?

12.6 *Photoelectrolytic cell efficiency* Assume that the hydrogen produced by the system in Fig. 12.9*c* and *d* is to generate electricity through the use of a fuel cell. Assume also that the efficiencies of electrolysis and of the fuel cell are both 70 percent. What do you estimate the sunlight-to-electricity conversion efficiency of this system to be?

12.7 *Invent a process* Suggest a procedure for producing photovoltaic cells (not photoelectrolytic cells) inexpensively by borrowing ideas from the procedure for producing the cell shown in Fig. 12.9*c*.

1

ANNOTATED BIBLIOGRAPHY

The most comprehensive source of information on photovoltaic developments is the published proceedings of the latest IEEE Photovoltaic Specialists Conference, an international conference held in the United States every eighteen months. Papers from the April 1979 West Berlin conference sponsored by the Commission of the European Communities appear in *Photovoltaic Solar Energy Conference,* R. Van Overstraeten and W. Palz, Eds. (Dordrecht, Netherlands, 1979).

Of the periodicals, *Solar Cells* (Elsevier-Sequoia, S. A., Lausanne, Switzerland) deals exclusively with photovoltaics. Some articles on PV phenomena and devices appear in applied physics and electronic device journals, such as *Journal of Applied Physics* (U.S.), *Applied Physics Letters* (U.S.), *Japanese Journal of Applied Physics, IEEE Transactions on Electron Devices* (U.S.), *Electronics Letters* (U.K.), *Journal of Physics D: Applied Physics* (Institute of Physics, U.K.), *Revue de Physique Appliqué* (France), and *physica status solidi (a)* (Akademie-Verlag, Berlin).

The *Journal of the Electrochemical Society* contains many articles on important processing technologies. The following journals on energy contain occasional articles about solar cells and their applications: *Energy Review* (International Academy, Santa Barbara, Calif.), *Energy Sources* (Crane, Russak and Co., New York), *Geliotekhnika* (Academy of Sciences, Uzbek, U.S.S.R. (English translation: *Applied Solar Energy*, Allerton Press, New York), *International Journal of Energy Research* (John Wiley and Sons, Sussex, England), *International Journal of Solar Energy* (Harwood Academic Publishers, New York), *Journal of Power Sources* (Elsevier-Sequoia, S.A., Lausanne, Switzerland), *Solar Energy* (Pergamon Press, Oxford, England, for International Solar Energy Society, Victoria, Australia), *Solar Energy Materials* (North-Holland Publishing Co., Amsterdam, Netherlands), and *Solar Engineering Magazine* (Solar Energy Industries Assoc., Washington, D.C.).

Abstract journals such as *Energy Research Abstracts* (DOE), *Electrical and Electronics Abstracts*, and *Physics Abstracts* are of course useful in searching the journal literature. Incidentally, the *Science Citation Index* permits one to find current references to specific previously published articles, and can be used to keep up to date on a particular topic.

Of the books on the subject, the 1976 IEEE reprint volume *Solar Cells*, edited by C. E. Backus, is noteworthy because of its selection of key articles published as the field developed.

Additional sources of interest are: *Application of Solar Technology to Today's Energy Needs* (Office of Technology Assessment, U.S. Government Printing Office, 1978), which surveys all solar technologies including PVs, and contains economic analyses of applications ranging from individual houses to small cities in specific locations; periodic government newsletters (such as DOE's "The Energy Consumer"); and the vast collection of reports of governmentally sponsored research and development projects (for U.S. work, contact SERI and consult the NTIS listings). Issued patents form a useful and often overlooked body of detailed and current information. Computerized literature-searching is possible in the journal abstract, NTIS report, and the U.S. patent databases.

The Solar Energy Information Data Bank, operated by SERI, is a U.S. national solar energy information network offering bibliographic and non-bibliographic database-searching capabilities; a national computer system for scientific computations, modeling, and simulation; and information dissemination services. Remote telephone access for machine searching is possible in the following databases: models, calendar of solar-related events, bibliographic entries, manufacturers' data, international projects and contracts, education, and solar legislation.

2

UNITS AND RELEVANT NUMERICAL QUANTITIES

PHYSICAL CONSTANTS

Boltzmann constant: $k = 1.38066 \times 10^{-23}$ J/K

Electron charge: $q = 1.60218 \times 10^{-19}$ C

Electron mass: $m_0 = 0.91095 \times 10^{-30}$ kg

Planck constant: $h = 6.62617 \times 10^{-34}$ J·s

Speed of light in vacuum: $c = 2.99792 \times 10^{8}$ m/s

Thermal voltage at 300 K: $kT/q = 0.0259$ V

Wavelength of 1-eV photon: 1.23977 μm

UNITS AND CONVERSION FACTORS

Energy:

1 kWh = 1000 Wh = 3.6×10^{6} J = 860.4 kcal = 3413 Btu

1 Btu = 2.93×10^{-4} kWh = 10^{-5} therm = 10^{-15} Q (quad)

Power:

1 MW = 1000 kW = 10^{6} W = 10^{6} J/s

1 kW = 0.239 kcal/s = 1.341 hp = 3413 Btu/h

Solar flux:

$$1\ \text{kW/m}^2 = 316.9\ \text{Btu/ft}^2\cdot\text{h} = 1.433\ \text{langley/min (cal/cm}^2\cdot\text{min)}$$

Time:

$$1\ \text{yr} = 365\ \text{days} = 8760\,\text{h} = 3.15 \times 10^7\ \text{s}$$

Length:

$$1\ \text{m} = 100\ \text{cm} = 3.281\ \text{ft} = 39.37\ \text{in}$$

$$1\ \text{mi} = 5280\ \text{ft} = 1.609\ \text{km} = 1609\ \text{m}$$

Area:

$$1\ \text{m}^2 = 10^4\text{cm}^2 = 10.76\ \text{ft}^2 = 1549\ \text{in}^2$$

$$1\ \text{acre} = 4047\ \text{m}^2 = 0.4047\ \text{hectare}$$

$$1\ \text{mi}^2 = 2.59\ \text{km}^2 = 2.59 \times 10^6\ \text{m}^2 = 640\ \text{acre}$$

Weight:

$$1\ \text{kg} = 1000\ \text{gm} = 2.205\ \text{lb}$$

$$1\ \text{ton} = 2000\ \text{lb} = 907.2\ \text{kg} = 0.9072\ \text{metric ton}$$

SOME RELEVANT ESTIMATES

Maximum solar insolation at sea level = $1\ \text{kW/m}^2$

Radius of earth = 6.4×10^6 m

World solar insolation (24 hr average) = 9.2×10^{16} W = $180\ \text{W/m}^2$

World energy consumption rate (1978) = 9×10^{12} W

U.S. energy consumption rate (1978) = 3.6×10^{12} W

World electricity consumption rate (1978) = 7.5×10^{11} W

U.S. electricity consumption rate (1978) = 2.6×10^{11} W

Approximate energy (heat) content in

1 metric ton coal = 8200 kWh

1 barrel oil = 1700 kWh

1 gallon gasoline = 40 kWh

1 cubic foot gas = 0.3 kWh

Approximate efficiency of oil/coal electric power plant = 35 percent.

4

ABBREVIATIONS AND ACRONYMS

AES Auger electron spectroscopy; quantitative analysis of atoms near surface of a solid obtained from energy spectrum of electrons reflected from an incident primary electron beam.

AM0, AM1, . . . air mass number; number characterizing intensity of sunlight at the earth, outside the atmosphere (AM0), at surface with sun directly overhead in clear sky (AM1), etc. (see Chap. 2).

AR antireflection; refers to transparent coating or coatings of proper thickness to reduce reflection of light from front surface of solar cell.

BOS balance-of-system; elements of PV power system other than cell array, concentrator, and tracking systems.

BSF back-surface field; type of solar cell in which heavy doping at unilluminated back surface causes charge carriers to be repelled, thereby increasing efficiency (see Chap. 3).

CIS conductor-insulator-semiconductor; composite solar cell structure having conductor separated by an insulating layer from semiconductor (see Chap. 11), similar to MIS.

CPC compound parabolic concentrator; nonimaging concentrator for solar cells employing parabolic reflecting surfaces set at an angle to each other (see Chap. 5).

CVD chemical vapor deposition; growth of solid layer on substrate in heated chamber supplied with gas containing atoms that form the layer.

CZ Czochralski; growth of large single-crystal ingot by slowly withdrawing a seed crystal in contact with molten material (see Chap. 4).

DLTS deep-level transient spectroscopy; determination of energy levels of trapping centers from, usually, the temperature dependence of the rate of decay of the capacitance of a *pn* or MOS capacitor made on the semiconductor under study, following a step change in the bias voltage across the capacitor.

DOE Department of Energy (U.S.); responsible for energy research and development.

EFG edge-defined film-fed growth; growth of (nearly) single-crystal ribbons, typically of silicon, for solar cells by solidification through a die (see Chap. 9).

EPI epitaxial (Gr.: *epi* = on, upon; *taxis* = arrangement); refers to growth of a crystalline film that nucleates with the correct orientation because of the spatial periodicity of the substrate.

ERDA Energy Research and Development Administration (U.S.); predecessor to U.S. Department of Energy.

FF fill factor; factor in solar cell efficiency, equal to current-voltage product at maximum efficiency divided by short-circuit current times open-circuit voltage (see Chap. 3).

FZ float zone; purification of semiconductor by heating so that a molten zone of the material passes through an ingot, taking impurities with it.

IBC interdigitated back contact; solar cell having electrodes on back instead of front surface to eliminate reflection or absorption of incident light.

IC integrated circuit; miniaturized solid-state electronic circuit.

IEE Institution of Electrical Engineers (U.K.); professional society.

IEEE Institute of Electrical and Electronics Engineers (U.S.); professional society.

ITO indium-tin oxide; large bandgap semiconductor employed as optically transparent electrode for conventional or Schottky-barrier solar cells.

LDC less-developed countries; nations other than the Western and the centrally managed economies, typically having relatively low per-capita incomes.

LED light-emitting diode; semiconducting *pn* junction, which emits light when electric current passes through it.

LPE liquid-phase epitaxy; growth of oriented crystalline solid film from a liquid in contact with an underlying substrate in a heated chamber.

MBE molecular-beam epitaxy; growth of solids layer-by-layer from beams of impinging atoms in an evacuated chamber.

MIS metal-insulator-semiconductor; similar to MOS, having metal and semiconductor separated by an insulator.

MOS metal-oxide-semiconductor; type of semiconductor device employing metal electrode separated by an oxide insulator from an underlying semiconductor.

NAA neutron activation analysis; quantitative determination of constituent atoms in a solid from their characteristic gamma-ray emissions following neutron bombardment.

NASA National Aeronautics and Space Administration (U.S.); responsible for U.S. space program.

NSF National Science Foundation (U.S.); responsible for U.S. support of basic research and development, primarily in universities.

NTIS National Technical Information Service (U.S.); distributes reports on U.S. government-sponsored research and development projects.

PEC photoelectrochemical; solar energy conversion involving use of liquid electrolyte and production of electricity and/or fuel gases (see Chap. 12).

PR photoresist; photon-sensitive emulsion used to delineate areas to be selectively etched away during fabrication of semiconductor devices.

PV photovoltaic; abbreviation used as in "PV system."

RBS Rutherford back-scattering; quantitative determination of atoms at or near the surface of a solid from the characteristic energy loss suffered in the back-scattering of a beam of incident alpha particles.

RTR ribbon-to-ribbon; crystallizing or enlarging grains in polycrystalline silicon ribbon stock by heating ribbon as it moves between supporting rollers (see Chap. 9).

SEM scanning-electron microscope; electron microscope that forms images of objects from secondary electrons produced by a scanned primary elctron beam.

SERI Solar Energy Research Institute (U.S.); organization in DOE responsible for solar energy research and development.

SHAC solar heating and cooling of buildings.

SIMS secondary-ion mass spectroscopy; quantitative determination of composition near surface of solid through mass spectroscopy of atoms sputtered away by impact of incident beam of ions such as argon.

SIS semiconductor-insulator-semiconductor; composite structure having typically one wide- and one narrow-bandgap semiconductor separated by insulator.

SOC silicon-on-ceramic; polycrystalline film obtained by cooling a ceramic sheet wiped with or dipped into molten silicon (see Chap. 9).

SPE solid-phase epitaxy; regrowth without melting of an amorphous layer upon underlying crystalline substrate, as in scanned laser annealing of semiconductors.

SPS satellite power system; proposed system having orbiting solar panels producing electricity beamed to earth on microwave beam for rectification and use (See Chap. 12).

SSMS spark source mass spectroscopy; quantitative determination of composition of a solid by mass spectroscopy of ions produced when sample is vaporized in a spark between inert electrodes.

STEP solar thermal electric power generation.

TPV thermophotovoltaic; process of producing electricity with solar cell illuminated by blackbody radiation from radiator heated by solar or thermal energy (see Chap. 12).

VGMJ V-groove multijunction; multiple-junction solar cell, for use with

concentrator, produced in part by V-groove anisotropic etching (see Chap. 11).

VMJ vertical multijunction; multiple-junction solar cell, for use with concentrator, having series-connected current-collecting junctions oriented parallel to direction of sunlight incidence (see Chap. 11).

VPE vapor-phase epitaxy; growth of solid films, upon an underlying solid substrate, from a vapor in a heated chamber.

5

TABULATION OF DEMONSTRATED CELL EFFICIENCIES BY CELL TYPE

Material	V_{oc}, V	J_{sc}, mA/cm^2	FF	η, %
Silicon	0.622	34.3	0.796	16.8
Silicon	0.731	1380	0.745	18.3
Silicon	0.783	15000	0.75	17.6
Silicon	0.621	36.5	0.806	18.3
Silicon	0.540	32.7	0.76	13.3
Silicon	0.585	31.9	0.74	13.8
Silicon	0.572	24.2	0.76	10.5
Silicon	0.522	28.1	0.79	11.5
Silicon	0.561	26.2	0.778	11.4
Silicon	0.50	15	0.63	5
Amorphous-Si	0.84	17.8	0.676	10.1
Amorphous-Si	0.880	13.1	0.57	6.6
Amorphous-Si	0.878	11.1	0.66	6.4
GaAs	0.97	25	0.81	20
GaAs	0.93	28	0.81	18.2
GaAs	1.05	270	0.85	23
GaAs	—	—	—	21
GaAs	0.95	23	0.78	17
GaAs	0.76	24.4	0.63	12
AlGaAs/GaAs	2.05	10.8	0.74	16.5
GaAs	0.56	22.7	0.67	8.5
Cu_2S/CdS	0.52	24.8	0.71	9.2
Cu_2S/ZnCdS	0.6	22.8	0.75	10.2
$CuInSe_2$/CdS	0.4	38	0.63	9.4
$CuInSe_2$/CdZnS	0.431	39	0.631	10.6
CdS/CdTe	—	—	—	10.5
CdS/CdTe	0.79	—	—	8
CdS/InP	0.63	15	0.71	12.5
InP	0.66	24.8	0.64	11.5
WSe_2	0.72	22.6	0.57	10.2
$MoSe_2$	0.65	25	0.56	9.4
CdTe	0.723	18.7	0.64	8.6
CdSe	0.57	23.8	0.48	6.5
CdSe/ZnSe/Au	0.6	20	0.45	5.0
CuTe/CdTe	0.59	13	0.63	4.8
Zn_3P_2	0.48	18	0.55	4.3
CuInS/$CuInS_2$	0.41	19	0.43	3.3
Merocyanine/Al	1.2	1.8	0.25	0.7

* For additional listings see Table 9.1 (on rapid silicon-growth techniques) and Table 10.3 (on thin-film cells).

Area, cm^2	Remarks	Ref. no.
2	p^+-n-n^+	1
2	41× concentration	1
0.4	500× concentration	2
2.8	MIS, active area	3
2.8	semicrystalline, MIS	3
4	edge-supported growth	4
5	silicon-on-ceramic	
11.4	ITO/semicrystalline	4
45	EFG (ribbon)	5
0.04	roller quenching	6
1.1	a-SiC/a-Si p-i-n	7
0.73	MIS	4
1.2	p-i-n	4
0.5	n^+-p-p^+ homojunction	4
1.5	AlGaAs/GaAs	8
1.5	AlGaAs/GaAs, 10×	8
—	AlGaAs/GaAs, 1000×	9
0.5	CLEFT	4
0.1	on Ge-coated Si	4
4.0	tandem cell	4
9	CVD thin film, MIS	4
1	solution ion-exchange	4
1	16% Cd, 84% Zn	4
1	evaporation	4
—	20% Cd, 80% Zn	10
—	thin film	10
—	electrodeposition	10
0.23	single crystal InP	11
—	PEC	4
—	PEC	4
—	PEC	4
0.02	electrodeposition, Au/CdTe	4
1	electrodeposition	4
0.01		12
6		12
1	Mg/Zn_3P_2, thin film	4
0.12		12
1		12

REFERENCES

1. Fossum, J. G., Nasby, R. D., Burgess, E. L. (1978), Conf. Record, 13th IEEE Photovoltaic Spec. Conf., 1294.
2. Frank, R. I., and Goodrich, J. L. (1980), Conf. Record, 14th IEEE Photovoltaic Spec. Conf., 423.
3. Green, M. A., et al. (1980), Conf. Record, 14th IEEE Photovoltaic Spec. Conf., 684.
4. Feucht, D. L. (1981), Conf. Record, 15th IEEE Photovoltaic Spec. Conf., 648.
5. Kalejs, J. P., et al. (1980), Conf. Record, 14th IEEE Photovoltaic Spec. Conf., 13.
6. Arai, K. I., et al. (1980), Conf. Record, 14th IEEE Photovoltaic Spec. Conf., 31.
7. Catalano, A., et al. (1982), Conf. Record, 16th IEEE Photovoltaic Spec. Conf., to be published.
8. James, L. W., Moon, R. L. (1982), *Appl. Phys. Lett.*, Vol. 26, 467.
9. Kaminar, N., et al. (1982), Conf. Record, 16th IEEE Photovoltaic Spec. Conf., to be published.
10. Conf. Record, 16th IEEE Photovoltaic Spec. Conf. (1982), to be published.
11. Bachmann, K. J., and Buehler, E. (1975), *Appl. Phys. Lett.*, Vol. 26, 229.
12. Barnett, A. M., and Rothwarf, A. (1980), *IEEE Trans. Electron Devices*, 615.

6

SOLAR CELL EXPERIMENTS

Of greatest interest to the user of a cell is the maximum power P_{max} that the cell can deliver to a resistive load under given conditions of illumination. Related to that are the maximum cell efficiency η_{max} and the load resistance $(R_L)_{max}$ for maximum power output. Also of interest are the short-circuit current I_{sc}, the open-circuit voltage V_{oc}, and the fill factor FF. One will want to observe the variation of output power with time during the day as the sun moves across the sky, and possibly also the effect of ambient temperature on cell output. The reader interested in a deeper understanding of solar cell operation may also want to verify the dependence of I_{sc} and V_{oc} upon intensity of illumination. Several experiments for measuring these charactistics are outlined here.

EQUIPMENT REQUIRED

For Experiment 1 you require only the following simple apparatus:

1. Solar cell. Single cells may be purchased from hobby shops or the suppliers listed in Appendix 8.
2. Digital or analog dc voltmeter and milliammeter, or multimeter. The internal resistance of the voltmeter should be at least 1000 Ω/V to permit measurement of open-circuit voltage.
3. Assorted resistors in the 1 to 150 Ω range.
4. Light source. The sun or a lamp may be used.
5. Hookup wire.

In addition to this equipment, used in measuring I_{sc}, V_{oc}, the entire *I-V* characteristic, cell output power, and the optimum load for maximum power

output, the simple curve tracer of Experiment 2 requires only a low-frequency oscilloscope having horizontal and vertical channels and a step-down transformer to reduce the 110- or 250-V line voltage to a few volts. For Experiment 3, on the dependence of I_{sc} upon intensity of illumination, you will require a light source such as a flashlight or a microscope illuminator that provides a fairly uniform, slightly diverging beam. A photographic exposure meter is useful but not necessary.

EXPERIMENT 1

Connect the solar cell and meter as shown in Fig. A6.1. The cell may be illuminated with sunlight or by artificial light from a lamp. With no load resistor connected and the voltmeter (or multimeter set on "dc volts") connected as shown, measure V_{oc}. With an ordinary silicon solar cell the value should be around 0.6 volts. Next connect the dc milliammeter (or multimeter set on "dc milliamperes") across the cell and read I_{sc}. The value will depend on the area of the cell and the intensity of illumination. For a typical 2 cm by 2 cm silicon cell in AM1 sunlight, I_{sc} should be around 120 mA. Multiply V_{oc} by I_{sc} to determine the maximum possible power the cell could provide if it had a "square" I-V characteristic.

To determine the output under different load conditions, connect different resistors R_L across the cell as shown. Values should range from 1 to 150 Ω. Measure and tabulate for each value of R_L the voltage across points A–B, and the current obtained by putting the milliammeter (or multimeter set on "dc milliamperes") in series with the load resistor R_L. Compute the power output $P = I \times V$ for each load resistance for which it occurs. The ratio of the maximum power to the total input power, given by the product of the intensity of illumination and the area of the cell, is an approximate value of the cell efficiency. (For a typical silicon cell this will be at most about 15 percent.)

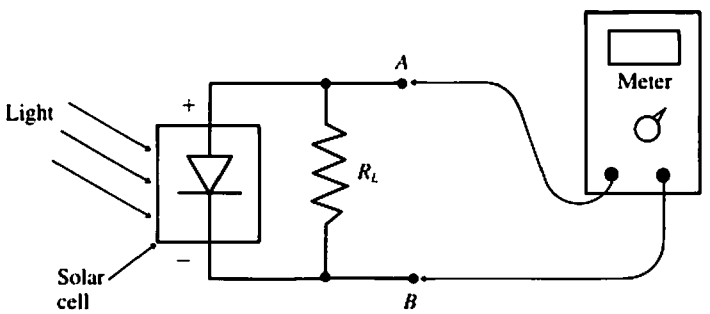

Figure A6.1 Set-up for Experiment 1.

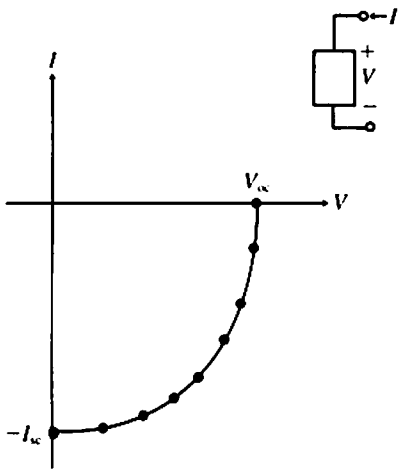

Figure A6.2 Typical plot of I vs. V for solar cell, taken with different load resistances R_L connected to cell. Note current and voltage conventions shown in inset.

For a more accurate value of the maximum efficiency, plot the pairs of values I and V you measure, draw a smooth curve through them (Fig. A6.2), and find the maximum power point. Note that with this method you will only obtain points in the fourth quadrant of the I-V characteristic, where the cell is delivering power to the load. The optimum load resistance for the cell will be $(R_L)_{max} = V_{max}/I_{max}$, where V_{max} and I_{max} are the voltage and current associated with the maximum power point. From the true maximum power, determine the maximum cell efficiency. Calculate the fill factor, $FF = P_{max}/I_{sc}V_{oc}$, which should be 0.7 or greater and is a measure of how "square" the I-V characteristic is.

EXPERIMENT 2

By using an oscilloscope having both horizontal and vertical input channels, you may display the I-V characteristics of solar cells quickly.

Connect the circuit shown in Fig. A6.3, using a step-down transformer to reduce the ac voltage from the mains to a few volts. Set the horizontal sensitivity to a volt or so per division, and display the voltage applied to the solar cell on the horizontal axis. The vertical deflection is proportional to the voltage across the series resistor R_S. If your oscilloscope has a vertical sensitivity of 10 mV per division, a 50-Ω resistor R_S will yield a 10-division vertical deflection if a 2-mA cell current flows. With the circuit connected as shown, the cell voltage will be displayed with positive values to the right, and the current with negative values upward. This simple curve tracer will display the entire I-V characteristic and the fourth quadrant will appear in the upper

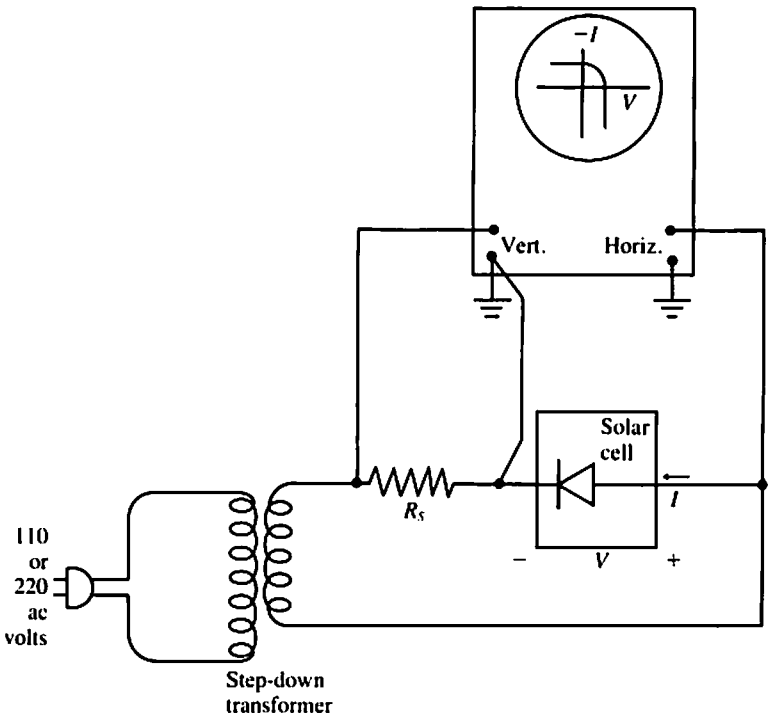

Figure A6.3 Circuit for using oscilloscope to display *I-V* characteristic of solar cell.

right corner of the screen. If you have a transistor curve tracer you can, of course, use it to display the *I-V* characteristics.

Connect the circuit and calibrate the display, finding the origin of the plot (all voltages off) and the vertical calbration (current = deflection in divisions × deflection sensitivity in volts per division ÷ R_S). Observe the *I-V* characteristic of the cell in the dark (this is the characteristic for a conventional *pn*-diode rectifier) and then gradually increase the illumination and note how the characteristic moves to increasingly negative currents as the photon-generated current from the cell increases.

EXPERIMENT 3

Using either the meters of Experiment 1 or the curve tracer of Experiment 2, you may observe the variation of the cell output with intensity of illumination.

Measure the short-circuit current each hour through the day with the cell illuminated by sunlight and oriented perpendicular to the sun at noon. Plot and interpret the results, considering that to the first order, I_{sc} is proportional to

the intensity of illumination and that the intensity reaching the interior of the cell decreases as the sun goes lower in the sky (air-mass number increasing) and as the angle of incidence of light on the cell increases.

If you have a way of measuring the intensity (see Chap. 2), you can calibrate your solar cell absolutely. Even without such equipment you may verify that I_{sc} is proportional to intensity of illumination, as follows.

Place a light source such as a flashlight or a microscope illuminator that projects a uniformly bright, slightly diverging beam, on a stable support. If you have a photographic exposure meter use it to determine two distances from the light at which the intensity differs by a factor of 2 (they are the distances at which the exposure meter readings differ by one f-stop or by a factor of 2 in shutter speed). Measure I_{sc} at each location and compare the values. If you do not have an exposure meter, you may use the following technique.

On a piece of cardboard draw two concentric circles whose *areas* are in the ratio of 1:2. Your solar cell should just fit inside the smaller circle. With the cardboard find the distance from the light source at which the beam just fills the larger circle, then place the solar cell there and measure I_{sc}. Now find with the cardboard the location closer to the light source where the beam just fills the smaller circle, and place the solar cell there and again measure I_{sc}. The intensity in the second location is approximately twice that in the first, and so the short-circuit current in the second case should be about twice that in the former.

OTHER EXPERIMENTS

You may see the deleterious effect of increasing temperature on cell performance by observing I_{sc} and V_{oc}, or the entire I-V characteristic as you *gently* heat the solar cell by bringing a soldering iron *near* its back surface. If you have a pulse generator and several light-emitting diodes (LEDs) you may be able to determine the effective minority-carrier lifetime in the cell by illuminating the cell briefly with light from the LEDs and observing the decay of I_{sc} after the light pulse ceases (values of a few to tens of microseconds are typically obtained with silicon cells). If you have colored filters with known transmission characteristics you can place them between the cell and the sun or a bright white light, such as an indoor movie light, and verify that the cell will not respond to very long wavelength radiation in the infrared portion of the spectrum. With a monochromator you can actually measure the wavelength at which response ceases and obtain an approximate value of the energy gap of the semiconductor used in the cell.

APPENDIX

7

COMPUTER SIMULATIONS OF PHOTOVOLTAIC CELLS AND SYSTEMS

A solar cell can be represented very roughly by a simple equivalent circuit containing a current source, a diode, and resistors, and the sun can be modeled as a blackbody at 5743 K. In a slightly more precise representation, such an equivalent circuit could be derived for each wavelength and the outputs of the circuits summed, each being weighted according to the relative intensity at that wavelength in the actual solar spectrum. But for serious exploratory solar cell studies and PV system development, such simple approaches are inadequate, and more comprehensive models and computer simulations are required. Three different types of computer program and data input are used:

Simulations of solar cell operation. These programs model mathematically the optical and electrical phenomena occurring in cells. When the cell dimensions and impurity distributions are provided along with solar spectral data, the typical program calculates the *I-V* characteristics, the efficiency and its components such as fill factor, and perhaps other quantities such as the excess carrier concentration at each point in the cell and the variation of cell output with temperature.

Economic and complete PV system simulations. Programs provide information ranging from the manufacturing costs for cells producing a given peak power under standard insolation to such quantities as average cost and annual energy production for cells at a particular location used with specified equipment for concentration, tracking, power conditioning, and energy storage.

Databases and special analysis programs. Examples are solar insolation data and electrical circuit and heat transfer analysis programs.

We shall discuss one particular solar cell simulation program, PERSPEC, as an example, and then comment on some other programs in the three categories. Incidentally, some programs may be available for distribution, but the reader is warned that even if programs have been written in a high-level language such as Fortran, they usually require some modification to run properly on a different computer, because of minor differences in compilers, operating systems, and subroutine libraries.

SIMULATIONS OF SOLAR CELL OPERATION

An example of a cell simulation program is the one-dimensional Fortran program PERSPEC, written by T. I. Chappell (1978). It combines multilayer optical simulation with semiconductor analysis to make a fast and accurate simulation program for photovoltaic solar energy converters. The program uses about 16,000 bytes of central computer memory with memory overlays, and requires about 2 seconds of execution time on a CDC-6600 computer to find the short-circuit current, open-circuit voltage, and the maximum-power point on the *I-V* characteristic of a typical silicon *p-i-n* photovoltaic device in AM1 sunlight. About half a minute is required for a device in 200X sunlight. The program has been used successfully to simulate several different types of solar cells and a special sensor for very intense sunlight (Chappell, 1976).

Table A7.1 lists features of this large program, which was based on the work of Gwyn, Scharfetter, and Wirth (1967) and Scharfetter and Gummel (1969). The user inputs the cell dimensions and doping profiles, and chooses the other items listed under item I in the table. The doping profiles may be obtained from analytic expressions, or from a process program such as SUPREM, which will output the impurity profile resulting from the use of any of several standard silicon integrated circuit fabrication procedures, such as oxidation or ion implantation. (For information about SUPREM, contact the Technology Licensing Office, Stanford University, Stanford, Calif.)

The PERSPEC program contains as data (item II of the table) the solar spectrum, and electrical and optical characteristics of silicon, such as carrier mobilities and diffusion constants, lifetime, as well as the real and imaginary parts of the indices of refraction of silicon and various AR materials. Equations or tables in the program represent the variations of these characteristics with temperature, local electric field, doping, and excess carrier concentrations.

The program first solves the optical problem (item III) to find the light intensity throughout the cell and, from that, the rate of optical generation of mobile carriers at each point. The entire cell is divided into about one hundred layers, with thinner layers near cell surfaces or interfaces where electric fields and carrier densities change most rapidly. The program solves numerically

Table A7.1 Features of the PERSPEC solar cell simulation program

I. User supplies these quantities:
   Cell thickness
   Cell doping profiles (spatial distribution of impurities)
   Description of antireflection coatings employed
   Metal backing on cell
   Assumed cell temperature
   Sunlight concentration factor

II. Program contains these data and represents these phenomena:
   AM1 solar spectrum
   Carrier mobilities in silicon, and their dependences on doping, excess carrier concentrations, electric field, and temperature
   Carrier lifetime and its dependence on doping; Auger recombination
   Real and imaginary parts of indices of refraction of silicon and various antireflection coating materials

III. Program solves these problems and equations:
   Reflection, transmission, and absorption of photons
   Spatial distribution of optically generated mobile carriers
   Nonlinear semiconductor carrier-transport equations
   Poisson's equation

IV. Printed or plotted output:
   Conversion efficiency, short-circuit current, open-circuit voltage, fill factor
   I and V at maximum power output
   Illuminated and dark I-V characteristics
   Spectral response
   Accounting for all optical and electrical energy losses
   Spatial distributions of mobile carriers and electric fields

the semiconductor carrier transport equations and Poisson's equation, relating change of electric field to local charge concentration, starting from a first approximation for electric fields based on the assumption that space charge is zero everywhere. A self-consistent solution is sought where the net electric current of holes and electrons just inside the silicon must equal the current flowing in or out of the cell terminals, and the electric field integrated through the cell must equal the terminal voltage of the cell. The final results are printed out or plotted.

This program and others such as that of Fossum (1976) and the two-dimensional program written at Purdue University (Schwartz, Gray, and Lundstrom, 1982) can be applied to a wide variety of cell designs. As more is learned about carrier behavior in different semiconductors and at high concentrations, that new information can be incorporated in these programs. With a change of certain numerical values and internally stored data and equations, a program written for silicon can be converted to apply to gallium

arsenide or other semiconductors. The flexibility of these programs, and the speed with which they enable one to try new cell designs, makes them invaluable tools in solar cell research and development.

ECONOMIC AND COMPLETE PV SYSTEM SIMULATIONS

SAMICS (Solar Array Manufacturing Industry Costing Standards) is a routine for calculating, with a computer program or as a manual procedure, the prices of manufactured PV modules. With it one can estimate prices that would result from use of particular fabrication techniques to make solar cells of given size using specified cell materials, electrodes, coatings, and encapsulants. SAMICS, accessed through the Jet Propulsion Laboratory (Pasadena, Calif.), has international applicability as only the standard data in it need be changed.

An example of a complete PV system program is that written at the Aerospace Corporation (1975), which yields estimates of the costs of solar electricity and its competitiveness with electricity from other sources to meet a time-varying demand. The modularity of this program is evident in Fig. A7.1. Historically correct electricity demand and direct solar insolation data may be entered via magnetic tape records. Each module or subroutine shown can be altered as one studies different concentrators, cells, or system configurations. Dashed lines in Fig. A7.1 represent flow of electricity from back-up generating plants into storage at night, and during or just before cloudy weather. Dotted lines show flow of power for array tracking and cell cooling.

Results of other simulations using different, possibly proprietary, PV system simulations have been reported in the *Proceedings of the IEEE Photovoltaic Specialists Conference*. Extensive results for PV and combined PV-thermal systems are tabulated in Volume 2 of OTA (1978). As a final example, the NASA-Lewis Research Center (Cleveland, Ohio), has developed a program that was used to design the Schuchuli village PV system (Chap. 7). The program calculates average PV cell output by month for a particular location. It also determines PV array size, tilt angle, and battery storage capacity to meet a given load profile. Inputs are average monthly values (EDS, 1968) of insolation, sky cover, precipitable water, and atmospheric turbidity, plus solar cell area, efficiency, and maximum-power voltage. The simulation includes provision for PV module degradation and random variations in insolation. Selection of the optimum array size and battery capacity combination can be modified by system considerations, such as physical limitations for the PV array or batteries, or by economic considerations.

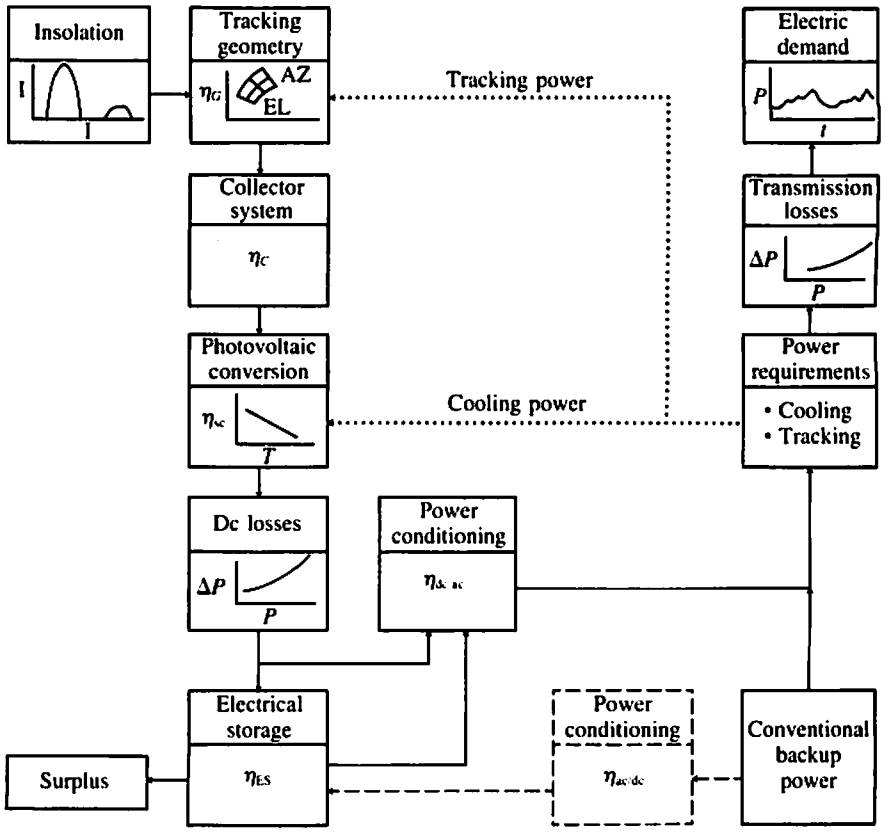

Figure A7.1 Photovoltaic system simulation model. In the plots, η = efficiency, AZ = azimuth, EL = elevation, I = direct solar insolation, P = power, ΔP = power dissipated resistively, T = temperature, and t = time.

DATA BASES AND SPECIAL ANALYSIS PROGRAMS

Data on the solar spectrum as obtained from measurements in space and corrected for absorption in the atmosphere have been published by ERDA (1977), as mentioned in Appendix 3. Measurements of intensity of sunlight have been made continuously for years at selected locations in the world. Questions about availability of insolation data for the United States should be directed to the DOE or SERI.

Standard electrical circuit analysis routines can be used to obtain *I-V* characteristics of lumped element equivalent circuits for solar cells. These routines range from circuit analysis modules run on small programmable

calculators to large, fast computer programs such as SPICE (for information, contact the Publication Office, Electronics Research Laboratory, University of California, Berkeley).

Finally, in studies of concentrator cells having complex shapes, one may wish to model heat flow—conduction, convection, and a linear approximation to radiative transfer—with a heat transfer program, such as the two-dimensional finite-element Fortran program HEAT (for information, contact Prof. R. L. Taylor, Civil Engineering Dept., University of California, Berkeley).

REFERENCES

Aerospace Corp. (1975), Mission Analysis of Photovoltaic Solar Energy Systems, Final Report, ATR-76(7476-01)-1, Vol. 2, El Segundo, Calif., December.

Chappell, T. I. (1976), A *pn* Junction Silicon Sensor for High Intensity Solar Flux Mapping, Proc., 12th IEEE Photovoltaic Spec. Conf., 760–763, November.

Chappell, T. I. (1978), The V-Groove Multijunction Solar Cell, Proc., 13th IEEE Photovoltaic Spec. Conf., 791–796; updated version in *IEEE Trans. Elec. Dev.*, Vol. 26, 1091–1097, July 1979.

EDS (1968), *Climatic Atlas of the U.S.*, U.S. Environmental Data Services, Washington, D.C.

Fossum, J. G., (1976), Computer-Aided Numerical Analysis of Silicon Solar Cells, *Solid State Electr.*, Vol. 19, 269–277, April.

Gwyn, C. W., Scharfetter, D. L., and Wirth, J. L. (1967), The Analysis of Radiation Effects in Semiconductor Junction Devices, *IEEE Trans. Nucl. Sci.*, Vol. 14, No. 6, 153–169, December.

OTA (1978), Application of Solar Technology to Today's Energy Needs, Office of Technology Assessment, U.S. Government Printing Office, June and September.

Scharfetter, D. L., and Gummel, H. K. (1969), Large-Signal Analysis of a Silicon Read Diode Oscillator, *IEEE Trans. Elec. Dev.*, Vol. 16, 64–77, January.

Schwartz, R. J., Gray, J. L., and Lundstrom, M. S. (1982), "The intensity dependence of surface recombination in high concentration solar cells with charge induced passivation," Proc., 16th IEEE Photovoltaic Spec. Conf., September (to be published).

8

SUPPLIERS OF SOLAR CELLS

Commercial suppliers of solar cells listed below are identified as follows:

[C-cell type] cells of type noted (Si, GaAs, CdS, conc.—for concentrator)
[S] entire PV systems (cells and arrays, equipment for power conditioning and storage, system control and monitoring)
[B] batteries for solar cell systems
[PC] power-conditioning equipment
[SP] cells for use in space environment
[O] other solar cell products

AEG-Telefunken, Industriestrasse 29, D-2000 Wedel (Holst.), Germany [C-Si, poly.-Si][S][SP]

ANSALDO, Via N. Lorenzi 8, 16152 Genoa, Cornigliano, Italy [C-Si][S]

ARCO Solar, Inc., 20554 Plummer, Chatsworth, CA 91311 [C-Si][B][PC]

Applied Solar Energy Corp., P. O. Box 1212, City of Industry, CA 91749 [C-Si, conc.][SP]

British Aerospace Dynamics Group, Filton, Bristol, BS127QW, England [SP]

Central Electronics Ltd., Site 4, Industrial Area, Sahibabad, U.P. 201005, India

Edmund Scientific Co., 5975 Edscorp Building, Barrington, NJ 08007

Energy Conversion Devices, Inc., 1675 W. Maple Rd., Troy, MI 48084 [C-amorphous Si]

Hughes Aircraft Co., Box 92919—Airport Sta., Los Angeles, CA 90009 [SP]

Japan Solar Energy Co., Kyoto, Japan

Kyoto Ceramic Co., 52-11 Inouecho, Higashino, Yamashina-ku, Kyoto, 607 Japan [C-Si][S]

Lockheed Missiles & Space Co., P. O. Box 504, Sunnyvale, CA 94086 [SP]

Martin Marietta, M.S. C0470, P. O. Box 179, Denver, CO 80201 [C-Si, conc.][S][SP]

Matsushita Electric, Kadoma, Osaka, Japan

Mobile Tyco Solar Energy Corp., 16 Hickory Dr., Waltham, MA 02154 [C-Si][S]

Nippon Electric Co., Japan

Optical Coating Laboratories, Inc., 2789 Giffen Ave., Santa Rosa, CA 95401 [C-Si][O-AR coatings]

Phillips Gloeilampenfabrieken, Elcoma Dept., Eindhoven, Netherlands [C-Si]

Photon Power, Inc., 1067 Gateway West, El Paso, TX 79903

Photowatt Intl., Inc., 2414 W. 14th St., Tempe, AZ 85281 [C-Si][S]

Poly Solar Inc., 2701 National Dr., Garland, TX 75041

Radio Shack, retail outlets throughout United States [C-Si]

RTC, Route de la Delivrande, 14000 Caen-Cedex, France

SEMIX, Inc., 15809 Gaither Rd., Gaithersburg, MD, 20760 [O-semi-crystalline silicon sheet for cells]

SES, Inc., Tralee Industrial Park, Newark, DE 18711 [C-CdS]

Sharp, 2613.1 Ichinomoto, Tenri-Shi, Nara, Japan [C][SP]

Solar Electric International, 4837 Del Ray Ave., Washington, D.C. 20014 [O-PV powered irrigation pumps]

Solar Generator, Singapore Pte. Ltd., 151 Loroug Chuan, Singapore, 1955 [C-Si]

Solar Power Corp. 20 Cabot Rd., Woburn, MA 01801 [C-Si][S]

Solar Usage Now, Inc., 450 E. Tiffin St., Basom, OH 44809 [C-Si][S]

Solarex Corp., 1335 Pickard Dr., Rockville, MD 20850 [C-Si][S][PC][B]

Solavolt International, 3646 E. Atlantic Ave., Phoenix, AZ 85062 [C-Si][S]

Solec International, Inc., 12533 Chadron Ave., Hawthorne, CA 90250 [C-Si][S]

Solectro-Thermo, Inc., 1934 Lakeview Ave., Dracut, MA 01836 [O-total energy systems (electrical and thermal output)]

Solenergy Corp., 171 Merrimas St., Woburn, MA 01801 [C-Si][S]

Spectrolab, Inc., 12500 Gladstone Ave., Sylmar, CA 91342 [C-Si, GaAs][S][SP]

Spire Corp., Patriots Park, Bedford, MA 01730 [C-Si, GaAs]

Tideland Energy Pty. Ltd., P. O. Box 519, Brookvale, N.S.W. 2100, Australia

Tideland Signal Corp., P. O. Box 52430, Houston, TX 77052 [S-solar-powered navigation aids]

Varian Associates, 611 Hansen Way, Palo Alto, CA 94306 [C-GaAs, conc.]

9

OVERVIEW OF SOME OPERATING SYSTEMS

The following tables summarize the operating characteristics of a number of remote stand-alone, residential, and intermediate load center PV systems (from J. L. Rease, "Photovoltaic Systems Overview", 14th IEEE Photovoltaic Spec. Conf., pp. 1139–1145, 1980).

Table A9.1 Remote stand-alone applications

User/application/ quantity/total watts/instal. date	Service	Operational period	Status
IHS/refrigerator/1/ 330/July 1976	Used by Papago Indian village for medical & food supplies at Sil Nakya, AZ.	Continous	A 12-ft^3 Magna-Kold refrigerator is being readied to replace the 4-ft^3 recreational vehicle refrigerator which has excessive run time in hot weather.
USFS/forest lookouts/2 588/October 1976	Antelope Peak, CA, and Pilot Peak, CA. Power for water, lights, radio and refrigerator.	May to October	Both lookouts closed for winter in late October. No problems. Dow Butte Lookout (north of Antelope Peak) equipped with PV system in October.
NOAA/weather station/5/ 481/April-August 1977	Halfway Rock, ME; Loggerhead Key, FL; Clines Corners, NM; Pt. Retreat, AK; South Pt., HI; RAMOS weather station power supply.	Continuous	Halfway Rock, ME, system became operational 9/25. One of the 3 strings in the PV array is noncontributing.
DOT/highway sign/1/116/April 1977	Power for receiver, transmitter, motor, and lights on changeable message, dust warning, sign near Tucson, AZ, on I-10.	Continuous	In operation.
USDA/insect survey traps/4/ 372/May 1977	Near Texas A & M in College Station, TX. Power for two black light and two electric grid insect survey traps.	April through September	Co-op experiment period completed. Disposition under review.

Lone Pine, CA/H_2O cooler/1/ 446/September 1977	Demonstration PV-powered water cooler for Owens Valley Interagency Committee Visitor Center, Lone Pine, CA.	Continuous	In operation.
NPS/refrigerator/1/ 220/July 1978	Food storage for back country ranger station in Isle Royale National Park, MI, wilderness area.	Summer 1976 Summer 1978 Summer 1979 Summer 1980	System removed for winter.
IHS-PTC/village power/1/ 3500/December 1978	Provide power to 95 people in Papago Indian village at Schuchuli, AZ, for water pump, 15 refrigerators, 47 lights, washing machine, and sewing machine.	Continuous	In operation.
NJ-DEP/air quality monitor/ 1/360/Nov. 1979	Demonstrate PV power for operation of high volume air sampler at Liberty State Park, NJ.	Continuous	In operation.
USGS/seismic sensors/1/40/Jan. 1980	Provide power to operate seismic instruments for Hawaii Volcanic Observation in Hawaii.	Continuous	In operation.

Table A9.2 Residential systems

Project	Operational	Array	Array code*	Inverter
Univ. of Texas/Arlington	Nov '78	6.2 kW_{pk} Sensor Tech Retrofit	G	Gemini 3 kVA
John F. Long Fiesta	June '80	4.5 kW_{pk} ARCO Solar	D	Gemini 8 kVA
Carlisle, MA ISEE	Feb '81	7.3 kW_{pk} Solarex	SO	Gemini 8 kVA
Molokai Wiepke House	Apr '81	4 kW_{pk} ARCO Solar	SO	Gemini 4 kVA
Pearl City	Apr '81	4 kW_{pk} ARCO Solar	SO	Gemini 4 kVA
Kalihi	Apr '81	2 kW_{pk} ARCO Solar	SO	Gemini 2 kVA
Florida Solar Energy Center	Nov '80	5 kW_{pk} ARCO Solar	SO	2-Gemini 4 kVA
MIT/LL NE Prototype	Dec '80	6.9 kW_{pk} Solarex	SO	Gemini 8 kVA
GE NE Prototype	Mar '81	6.1 kW_{pk} GE Shingle	D	Abacus 6 kVA
Solarex NE Prototype	Feb '80	5.3 kW_{pk} Solarex	SO	Abacus 6 kVA
TriSolar Corp. SW Prototype	Apr '81	4.8 kW_{pk} ASEC	I	Gemini 8 kVA
Westinghouse NE Prototype	Feb '81	5.4 kW_{pk} ARCO Solar	I	Abacus 6 kVA
TriSolar Corp SW Prototype	Apr '81	4.6 kW_{pk} ASEC	I	Gemini 8 kVA
Westinghouse SW Prototype	Apr '81	5.4 kW_{pk} ARCO Solar	I	Abacus 6 kVA
GE SW Prototype	June '81	5.6 kW_{pk} GE Shingle	D	Abacus 6 kVA
ASI SW Prototype	TBD	5.9 kW_{pk} ARCO Solar	D	Gemini 8 kVA
BDM SW Prototype	Apr '81	4.3 kW_{pk} Motorola	SO	Abacus 6 kVA
ARTU SW Prototype	TBD	4.9 kW_{pk} ARCO Solar	SO	TBD
Solarex SW Prototype	Apr '81	4.8 kW_{pk} Solarex	SO	Abacus 6 kVA
TEA SW Prototype	Apr '81	3.7 kW_{pk} Motorola	R	Abacus 6 kVA

* Array code: G—ground mount, D—direct mount, SO—stand-off mount, I—integral mount, R—rack mount.